Norwegian University
of Life Sciences

Master's Thesis 2024 30 ECTS
Faculty of Science and Technology - Department of Physics

Energy Yield Assessment of Floating Solar PV on Inland Water Bodies in Norway

Mette Lie
Environmental Physics and Renewable Energy

Preface

The journey to explore the potential of Floating Photovoltaic (FPV) systems in Norway has been an exhilarating adventure. This research would not have been possible without the support and contributions of many wonderful individuals and organizations, and it is my pleasure to extend my heartfelt thanks to them.

First and foremost, I owe a huge debt of gratitude to my academic advisor, Arnkell Jonas Petersen. Your continuous guidance, insightful feedback, and unwavering support have been the pillars upon which this research stands. Your expertise has been like a beacon, lighting the way through the complexities of this project. The same goes for my external co-supervisor, Stanislas Merlet from Multiconsult. It has been a pleasure getting to know you and your colleagues. Your fresh perspectives and practical insights have added immense value to this research. Collaborating with you has been both enlightening and enjoyable.

To my incredible coworkers at Elhub, thank you for infusing my days with enthusiasm and motivation. Hans Erik Budde, Jan Magne Strand, Frode Kaspersen, and Alexander Stokke Hammer-Dybvad, your engagement and support have been instrumental. Special thanks to Sigbjørn Høgne for not only providing office space but also for those luxurious lunches that kept me going.

I have to thank Misganu Debella-Gilo for his experience in GIS. By guiding me through unknown territory, he has played a significant role in the successful completion of the spatial analysis. I also want to thank Torunn Kjeldstad, Mari Benedikte Øgaard, Espen Olsen, Martin Brunstad Høydal, and Kristin Reitan for the valuable conversations that have enriched this research. Your insights and perspectives have been incredibly helpful.

To my family and friends, your unwavering support and encouragement have been my rock throughout this journey. A special thanks to my good friend, Monty Hatfield, for his boundless enthusiasm and constant presence. Your patience and understanding have been a wellspring of strength and motivation.

I am also very grateful for the financial support from the master's program, making it possible for me to attend the Norwegian Solar Cell Conference (NSCC) 2024. This opportunity allowed me to meet new people in the solar industry, further expanding my knowledge and network in this exciting field.

But nothing of this could be achievable without quality data. A huge gratitude goes to the Norwegian Water Resources and Energy Directorate (NVE) for offering lots of valuable datasets, openly available to everyone, setting the groundwork for various analyses, and significantly enriching the quality and depth of this research.

I hope that the findings and insights presented in this report will not only contribute to the advancement of renewable energy solutions but also inspire future research in the field of FPV systems.

Mette Lie
Norwegian University of Life Sciences (NMBU)
Faculty of Science and Technology - Department of Physics
May 15, 2024

Abstract

The pursuit of sustainable energy sources has become increasingly critical in addressing global climate change. The Norwegian parliament's revised budget plan for 2023 set a target for new solar energy at 8 TWh by 2030. Floating photovoltaic (FPV) systems offer a solution by utilizing bodies of water, easing the installation process, and enabling deployment near demand sites, reducing the overall project timeline. FPV might therefore be an interesting choice to meet 8 TWh by 2030.

Despite Norway's abundant water resources and increasing focus on sustainable energy solutions, the feasibility and impact of floating photovoltaic (FPV) systems in the country have not been thoroughly assessed. This study aims to fill this gap by investigating the potential of FPV systems as a renewable energy solution in Norway.

This study explores the potential of floating photovoltaic (FPV) systems as a renewable energy solution in Norway. Leveraging geospatial and weather data, five scenarios were investigated, focusing on lake surface with proximity to grid connection as potential FPV installation sites.

Results indicate that FPV systems have substantial potential to contribute to Norway's renewable energy goals, especially when located at hydro power reservoirs. The study found that covering 25% of hydro power, has the potential to generate 20.4 TWh, while not exceeding the installed capacity of the hydro plant. By harnessing the power of Norway's water bodies, FPV systems offer a promising pathway towards a more sustainable energy future.

Key challenges identified include grid connectivity, environmental impacts, and higher operational costs compared to land-based systems. Despite these challenges, FPV systems present a viable solution to increase local solar energy production, reduce land use conflicts, and improve energy security. Future research should focus on optimizing FPV designs for Nordic conditions, addressing environmental impacts, and exploring economic incentives to promote investment.

Sammendrag

Jakten på bærekraftige energikilder blir stadig viktigere for å møte de globale klimaforandringene. I Stortingets reviderte budsjettplan for 2023 ble det satt et mål om å produsere 8 TWh ny solenergi innen 2030. Flytende solcelleanlegg (FPV) representerer en lovende løsning ved å utnytte vannflater, forenkle installasjonsprosessen og plassere solcelleanlegg nær forbrukssteder, noe som kan redusere prosjektets totale tidslinje betydelig. FPV kan derfor være en nøkkelteknologi for å nå dette målet.

Til tross for Norges rikelige vannressurser og økende fokus på bærekraftige energiløsninger, er gjennomførbarheten og effekten av flytende solcelleanlegg (FPV) i landet ikke grundig vurdert. Denne studien har som mål å fylle dette gapet ved å undersøke potensialet til FPV-systemer som en fornybar energiløsning i Norge.

Studien utforsker potensialet for flytende solcelleanlegg som en fornybar energiløsning i Norge. Ved å utnytte geospatiale data og værdata ble fem scenarier undersøkt, med fokus på innsjøoverflater med nærhet til nettilkobling.

Resultatene indikerer at FPV-systemer har betydelig potensial til å bidra til Norges fornybare energimål, spesielt når de er plassert ved vannkraftreservoarer. Studien fant at dekking av 25% av overflatene på vannkraftreservoarer har potensial til å generere 20,4 TWh, uten å overskride den installerte kapasiteten til vannkraftverket. Ved å utnytte kraften fra Norges vannflater, tilbyr FPV-systemer en lovende vei mot en mer bærekraftig energifremtid.

Nøkkelutfordringer som ble identifisert inkluderer nettilkobling, miljøpåvirkninger og høyere driftskostnader sammenlignet med landbaserte systemer. Til tross for disse utfordringene presenterer FPV-systemer en levedyktig løsning for å øke lokal solenergiproduksjon, redusere konflikter om arealbruk og forbedre energisikkerheten. Fremtidig forskning bør fokusere på å optimalisere FPV-design for nordiske forhold, adressere miljøpåvirkninger og utforske økonomiske insentiver for å fremme investeringer.

Contents

Nomenclature

Symbols

β	Temperature coefficient
T_{amb}	Ambient temperature (K)
T_{mod}	Module temperature (K)
G	Global irradiance (W/m^2)
P	Electrical power (W)
U-value	Heat transfer component

Abbreviations

AM	Air mass
AOI	Angle of incidence
FPV	Floating photovoltaics
IAM	Incidence angle modifier
NVE	The Norwegian Water Resources and Energy Directorate
PV	Photovoltaics

Subscripts

amb	Ambient
b	Bandgap
cond	Conduction
conv	Convection
i	Incident
ph	Photon
POA	Plane of array
r	Reflected
rad	Radiance
STC	Standard test conditions
t	Transmitted

1 Introduction

In the 2023 revised budget plan, the Norwegian parliament set an ambitious target of generating 8 TWh of new solar energy by 2030. To achieve this goal, the government was tasked with developing a concrete action plan by 2024. [1]

In response to this, the Norwegian Water Resources and Energy Directorate (NVE), working on behalf of the Ministry of Energy, has conducted a thorough assessment to determine what is required to achieve 8 TWh of solar power by 2030 [2]. NVE recommends that the threshold for concession requirements for solar power facilities be set at 5 MW [2], making it easier to establish local solar energy production and shortening the investment process.

In 2023, Norway's electric solar energy generation totaled 0.17 TWh [3]. Reaching 8 TWh by 2030 would need a significant acceleration in solar energy installations. However, installations located at a considerable distance from the areas of energy demand have longer construction times and higher investment costs, particularly if extensive high-voltage transmission infrastructure is necessary [4]. Establishing local land-based solar farms can be challenging due to the need for large areas of land, which often compete with agriculture and urban expansion [5].

Floating photovoltaic (FPV) systems have gained attention for their innovative approach to local solar energy generation. By harnessing solar power on bodies of water, FPV systems bypass the competition for land resources typically encountered by land-based solar farms, making them an attractive option for regions where land availability is limited or prioritized for other uses such as urban expansion or agriculture [4].

Moreover, the cooler environment provided by water bodies can enhance module performance by reducing cell temperatures, thereby improving overall energy output. This combination of benefits positions FPV as a compelling contender to fulfill the growing energy demands of the future.

Norway's extensive experience in maritime, offshore, and energy industries, combined with its ability to handle rough weather conditions, positions the country well to lead technological advancements in FPV systems [6], [7]. Norwegian companies like Ocean Sun and Sunlit Sea have already developed FPV technologies, and Ocean Sun are producing FPV installations internationally [8], [9].

1.1 Motivation

Despite Norway's abundant water resources and increasing focus on sustainable energy solutions, the potential of floating solar power remains largely unexplored. To the best of the author's knowledge, there has not been a thorough assessment of whether FPV technology could significantly impact Norway's renewable energy sector.

Meeting the ambitious 8 TWh target by 2030 necessitates swift action in deploying renewable energy infrastructure. However, there are multiple factors that increase the projects timeline, some being grid connectivity, applications and regulations. For a project to be approved by the municipality, it cannot occupy a nature-reserved area, or be within a flood-hazard area.

As of now, there are no regulations on how much of the lake surface it is allowed to cover. This would depend on local factors such as the value that the lake contributes to the community. For aggregated studies, such as finding the total potential of FPV deployment in countries, continents, or on a global level, it has been common to investigate 100%, 25%, and 10% coverage.

The motivation for this study is to address the knowledge gap of the potential of FPV deployment on Norwegian lakes and evaluate the role that FPV systems can play in Norway's renewable energy investment in near future.

1.2 Objective

The objective of this work is to determine the potential energy yield of floating photovoltaic (FPV) systems in Norway, with a focus on local production sites. Five scenarios are investigated, starting with a maximum coverage scenario to estimate the highest possible energy yield. Following this, a socially acceptable scenario is established by excluding conserved and flood hazard areas and limiting the coverage to 10%. The study also examines the potential for local FPV deployment to contribute to the 8 TWh target by leveraging the Norwegian Water Resources

and Energy Directorate's recommendation of a 5 MW threshold for concession requirements. Lastly, the potential of combining hydro plants with solar plants is investigated, considering constraints on reservoir coverage and installed capacity.

This methodology is an attempt to not only understand the total potential but also the potential that can realistically be achieved in the near future without incurring large investments in net infrastructure.

Based on the stated objectives, this report will focus on the following research questions.

- How does a solar cell function?
- How does FPV compare to land-based PV systems?
- What challenges do FPV face in Nordic climates?
- What is the extent of the total lake surface in Norway, and what is the annual energy yield when covering 100 % of it?
- To what degree are FPV installations socially accepted, and what is the annual energy yield potential?
- What are the practical factors limiting FPV installations in the near future?
- How much energy can potentially for near future installations without large investments in net infrastructure?
- How much energy can be harnessed from reservoirs that is already used for hydroelectric purposes?

Due to the time constraint of 4.5 months, these topics are not covered in detail:

- How mechanical technology and the system efficiency is affected by meteorological impacts such as current, waves, wind, snow and ice.
- The cost of installing and operating a floating PV system.
- The environmental risk.
- Validation of the data and model used for estimation.
- Comparison of efficiency with respect to other technologies.
- The microclimatic conditions at lake surface level.

2 Theory

This chapter provides the theoretical foundation for analyzing floating photovoltaic (FPV) systems in the context of Norwegian lakes. The chapter will start by unraveling the principles of solar irradiance and the functionality of solar cells, before diving deeper into the challenges and advantages associated with FPV installations, including considerations like cooling effects, installation processes, and environmental impacts. The theory section 2.1-2.2.2 and 2.8 is based on *Solar Energy - The physics and engineering of photovoltaic conversion technologies and system*, unless other sources are specified.

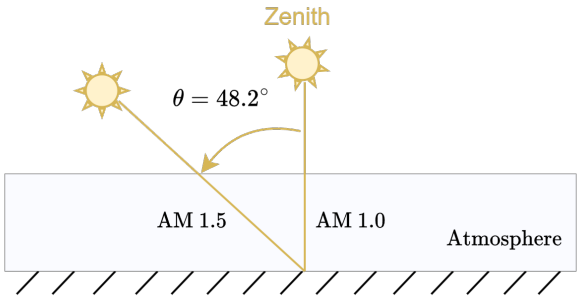

Figure 1: Solar irradiance penetrating the atmosphere at zenith angle 0 and 48.2°.

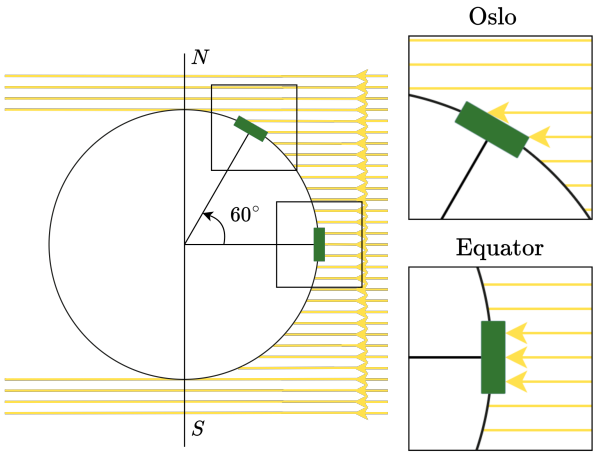

Figure 2: Simplified illustration of how sunlight hits the earth's surface at midday on a spring or autumn day [10]. The density of sunlight hitting Oslo is approximately 50% of sunlight hitting the equator. Inspired by [10]

2.1 Solar irradiance

Solar irradiance is the amount of solar energy received per unit area. The average solar irradiance at the outer boundary of Earth's atmosphere is approximately 1.361 $\frac{W}{m^2}$. However, as light travels through the atmosphere to the Earth's surface, it interacts with gases and particles, affecting the irradiance that reaches the surface. High-energy photons with shorter wavelengths are scattered more strongly by atmospheric molecules, while low-energy photons are less affected. Consequently, the intensity of solar irradiance at the Earth's surface depends on the distance traveled through the atmosphere and varies for each wavelength.

The spectrum outside the atmosphere is referred to as the AM0 (Air Mass Zero) spectrum because the light has not passed through any air mass. AM1 is defined when the light has traveled through one atmosphere (Figure 1). The air mass can be calculated using the equation:

$$AM = \frac{1}{cos\theta}, \tag{1}$$

where θ is the solar zenith angle, defined as the angle between the solar irradiance and the axis perpendicular to the earth's surface.

Determining the irradiance per square meter of land or water surface involves projecting the irradiance from the area perpendicular to the incident light down to the surface [10]. As illustrated in Figure 2, higher latitudes exhibit a steeper surface tilt. This inclination results in the distribution of irradiance cross-section over a larger area, impacting the amount of irradiance per unit surface area.

2.1.1 Angle of incidence - AOI

When sunlight strikes the surface of a solar panel, some of it is reflected off the surface, while the rest is transmitted into the panel, as demonstrated in Figure 3. The amount of reflection and transmission depends on the angle of incidence, the polarization of light, the wavelength, and the refractive indices of the materials involved [11], [12]. A lower angle of incidence results in a higher proportion of refracted rays [12].

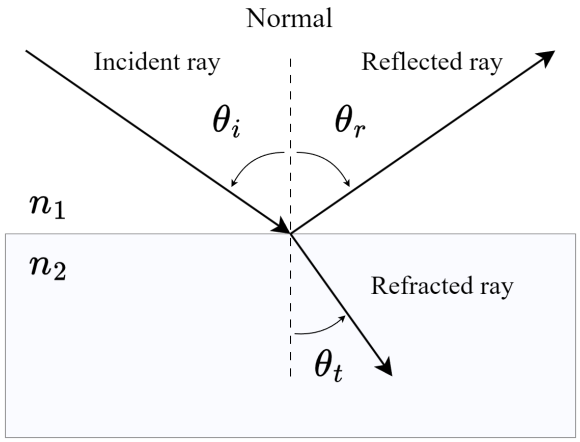

Figure 3: Incident ray coming in at an angle θ_i is reflected at an angle $\theta_r = \theta_i$ and refracted with angle θ_t. Both the angle and the amount of refracted ray is dependent on the incident angle θ_i, wavelength, and the refractive index of substance 1 and 2 (n_1 and n_2) [12]. Recreated from [11].

2.2 Functionality of a solar cell

When light strikes the solar cell, it is either reflected, transmitted, or absorbed by the semiconductor within the solar cell. A semiconductor is a type of material that has the property of conducting when the electrons are given enough energy to free themselves from the atoms. When an electron is freed from an atom, it leaves an unfilled space in the atomic structure, referred to as a hole. This process, called the generation of an electron-hole pair, is fundamental to the operation of a photovoltaic (PV) cell.

At room temperature, there will always be some thermal-generated electron-hole pairs. Radiative generation, on the other hand, occurs when an electron is excited by a photon with sufficient energy. The recombination of the electron-hole pair typically occurs within milliseconds, releasing energy in the form of photons or energy transfer to neighboring electrons, or lattice vibrations.

To prevent the electron-hole pair from recombining immediately, the solar cell is designed so that when a photon generates an electron-hole pair, an electric field separates the electron from the hole. This field is often created internally by the structure of the semiconductor. The separation of the positive and negative charge, holes, and electrons, creates a voltage difference between the front and the rear side of the cell.

Connecting the sides to an external circuit allows the electrons to travel through the circuit and reconnect with the holes without crossing the electric field in the wrong direction, as illustrated in Figure 5. Attaching an external load to the circuit makes it possible to utilize the voltage difference between the front and the rear side.

2.2.1 Shockley-Queisser Limit

Solar irradiance consists of a spectrum of photons with different energy levels. However, not all wavelengths contribute to electron-hole pair generation. The amount of energy required to free an electron from its atom depends on the semiconductor material. For instance, a single-junction crystalline silicon solar cell has an average bandgap of 1.12 eV, meaning it takes 1.12 eV to free an electron from its atom.

In relation to this criterion, there are two principal losses that reduce the efficiency of single-junction solar cells; photon absorption losses and thermalization losses. The first principle is that photons with energy below the bandgap threshold do not generate electron-hole pairs; instead, they are either transmitted or absorbed by the material structure. The second principle is that photons can only free one electron each. The excess energy of photons with energy above the bandgap is dissipated as heat during the thermalization process.

The thermalization process occurs when a high-energy electron interacts with the lattice atoms, transferring its excess energy, causing the atoms to vibrate more vigorously and thus increase the overall temperature of the material [13]. The process of thermalization occurs rapidly, typically within 10^{-12} seconds after the absorption of the photon.

2.2.2 Cell temperature

The performance of a PV module depends significantly on the temperature of the solar cells. Higher temperatures reduce the module's voltage, thereby decreasing output power and overall performance.

The cell temperature is highly influenced by irradiance and heat exchange with the environment [14]. The intensity of solar radiation directly affects the temperature of PV modules by increasing the thermalization within the cells. Additionally, heat exchange

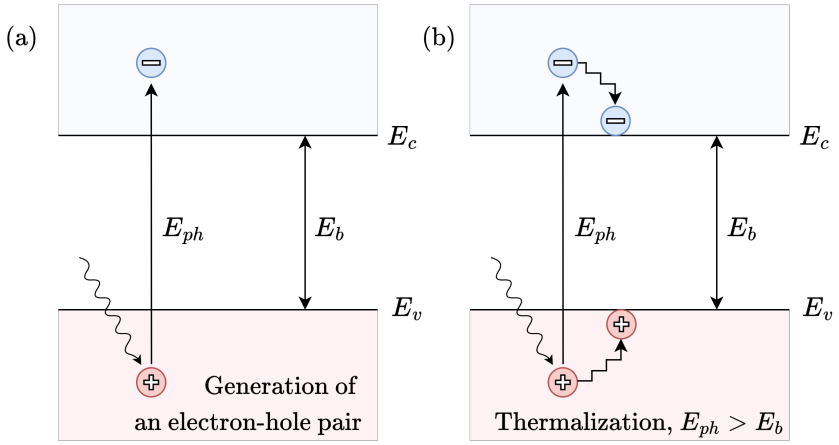

Figure 4: (a) A photon with energy E_{ph} excites an electron (-), leaving a hole in the atomic structure (+). (b) Thermalization occurs when $E_{ph} > E_b$ and the excess energy is dissipated as heat. Recreated from [11]

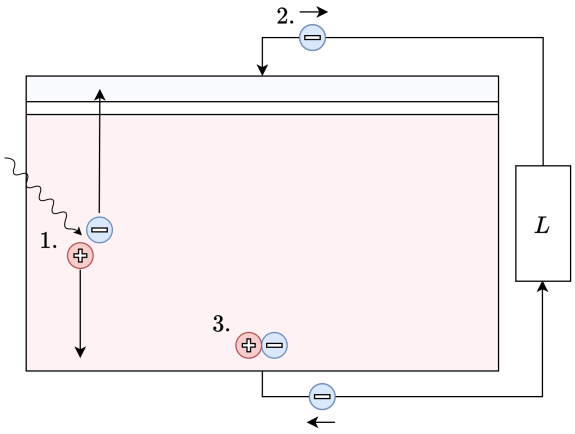

Figure 5: 1) A photon generates an electron-hole pair before an electric field separates them. 2) The electron flows through the circuit and loads to meet the hole at the rear side. 3) The electron and hole recombine, releasing energy. Inspired from [11]

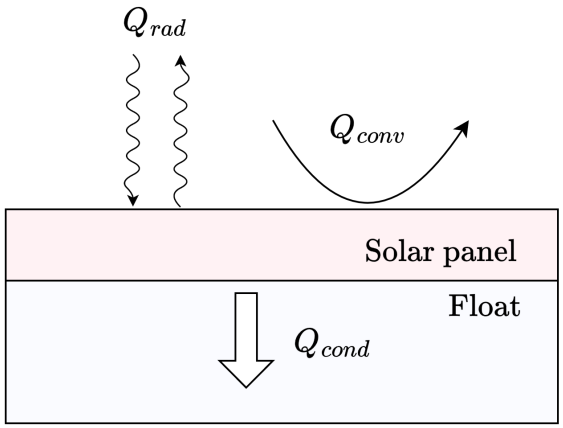

Figure 6: Illustration depicting the heat transfer processes between a solar panel and the surrounding environment. The components include radiated (Q_{rad}), convective (Q_{conv}), and conductive (Q_{cond}) energy. This visualization is inspired by the work presented in [15]

with the surrounding environment plays a significant role. Effective heat dissipation mechanisms are crucial to managing module temperatures and optimizing overall efficiency.

As illustrated in Figure 6, there are three primary mechanisms through which modules exchange heat. The first mechanism involves thermal conduction, wherein heat is transferred through direct contact with an element. The second mechanism, thermal radiation, occurs as electromagnetic waves emitted by the module's surface carry heat energy away. The third mechanism, convection, is when heat is transferred by moving fluid such as air or water [15].

2.3 Floating PV in general

The layout of a floating photovoltaic (FPV) system closely resembles that of land-based PV installations, with the primary distinction being the mounting of PV arrays and inverters on a floating platform, as illustrated in Figure 7. For small-scale FPV plants situated near the shore, inverters can be positioned on land [5].

Currently, most installations are situated in rel-

atively small and tranquil inland waters, including industrial basins, drinking water reservoirs, irrigation ponds, or sand-extraction ponds [16]. However, there is a growing trend towards establishing installations in more challenging environments, such as hydroreservoirs and expansive water bodies with rougher conditions [16].

Since the first system was established in 2007 in Aichi, Japan, a number of FPV technologies have been developed during its short time of existence, and the number is growing rapidly [5] [14].

The majority of FPV systems are mounted on HDPE floats, as illustrated in Figure 8 [4].

To address environmental concerns and enhance heat conductivity, some FPV systems utilize aluminum floats instead of traditional plastic materials (Figure 10). These aluminum floats offer improved durability and thermal performance, resulting in more efficient FPV installations [9].

Another innovative approach uses flexible membranes that enable the FPV modules to directly interface with the water surface, enhancing the cooling effect of the panels (Figure 9) [14].

Certain FPV systems integrate tracking mechanisms that dynamically adjust solar panel orientation to align with the sun's path throughout the day (Figure 11). While this optimization maximizes solar energy capture and enhances overall energy yields, it also adds complexity to the mooring systems [19].

2.4 Advantages of floating PV

Floating PV systems offer various advantages that make them an attractive option for solar energy generation. This chapter explores several of these advantages, including their cooling effect, efficient installation process compared to land-based PV, environmental benefits, and benefits when combined with hydroelectric and drinking water reservoirs.

2.4.1 Cooling effect

Maintaining low surrounding surface temperatures is crucial as it influences ambient temperature and the surrounding heat radiation levels. Unlike land, water allows solar radiation to penetrate beyond the surface layer, resulting in a cooler surface where the interaction with the PV module occurs. Water, having a higher specific heat capacity compared to air, land, and building materials, requires more energy to change its temperature, making it more resilient to temperature fluctuations. Additionally, the unrestricted movement of water allows heated water to blend with cooler water, promoting stability in surface temperatures throughout the day. [16]

Research conducted in 1981 by Griffith JS, Rathod NS, and Paslaski J. indicates that the temperature rise of photovoltaic (PV) cells relative to the ambient temperature is highly responsive to changes in wind speed, moderately influenced by wind direction, and minimally sensitive to changes in atmospheric temperature [20].

The wind speed profile is highly dependent on the roughness of the surface, as illustrated in Figure 12. Generally, the rougher the surface, the slower the wind speed is closer to the ground due to frictional effects with the surface obstacles [22]. Consequently, wind speeds are typically higher over water, which enhances convective heat exchange.

2.4.2 Installation process

Floating PV systems offer distinct advantages over land-based installations, particularly in terms of the installation process. Unlike land-based PV systems, FPV systems has no need for landscape modification, making the installation process notably quicker and more straightforward [5]. Installing FPV systems near demand centers is typically easier compared to land-based systems. The escalating land demand in urban regions not only inflates land prices but also imposes opportunity costs for land-based PV [5].

Even in areas where land is available for land-based PV installations, there's often a considerable distance between the energy generation site and the area of consumption. Transmitting solar energy over long distances via high-voltage lines can be costly and increase losses along the transmission path.

By situating power plants closer to consumers, the need for long-distance energy transmission is minimized, consequently reducing installation cost, environmental impact, and energy loss [5]. Having electric connectivity during the construction process may reduce the need for diesel aggregates [4].

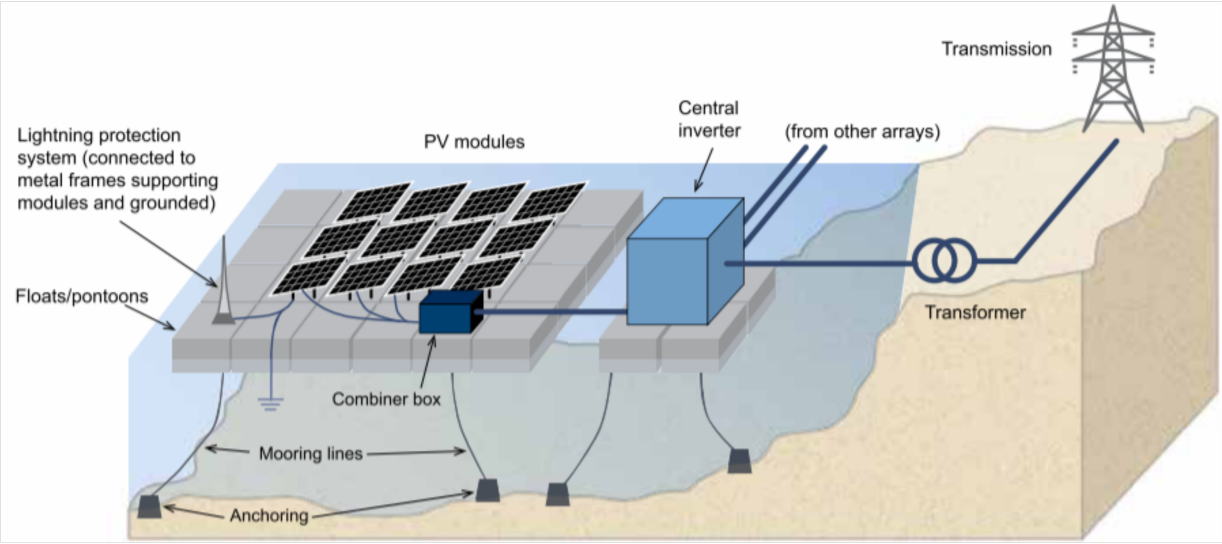

Figure 7: Key-components of a typical large-scale FPV system. Source: Solar Energy Research Institute of Singapore [5]

Figure 8: Tilted air cooled panels on plastic floats from SunEvo Solar. Source: SunEvo Solar [17].

Figure 10: Horizontal panels on aluminium floats from Sunlit Sea. With permission from [9].

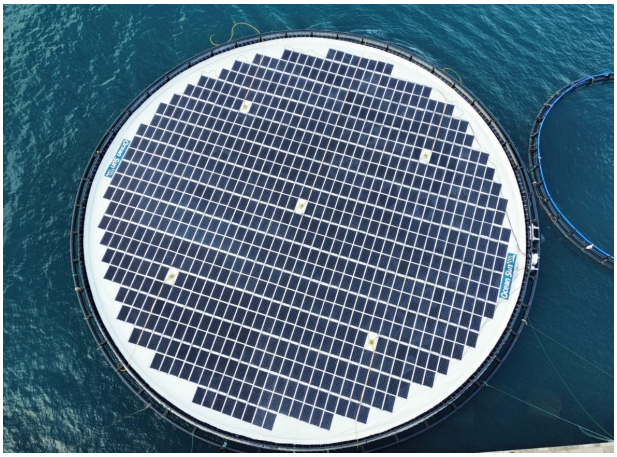

Figure 9: Horizontal water cooled panels on floating membrane from Ocean Sun. With permission from [8].

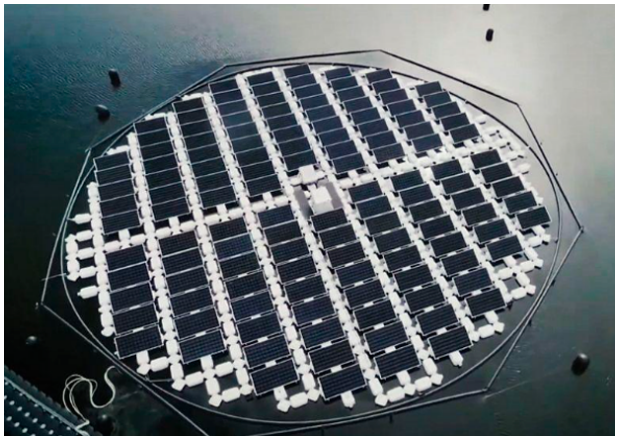

Figure 11: Tracing FPV panels from SolarisFloat. Source: SolarisFloat [18].

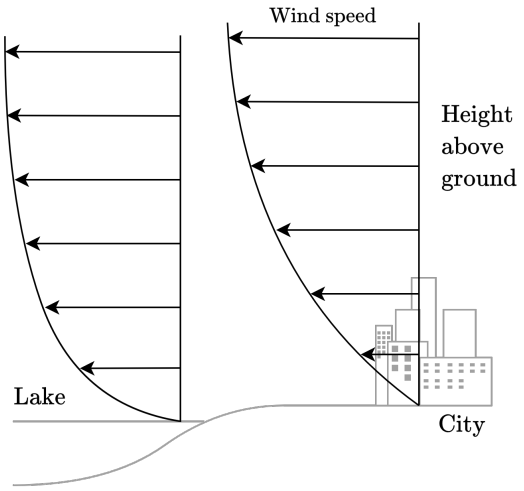

Figure 12: Wind speed gradient above lake and city. Inspired by [21].

2.4.3 Environmental advantages

There is a growing global concern about the increasing presence of toxin-producing cyanobacteria (blue-green algae) in water sources. These blooms can become problematic for both drinking water supplies and recreational water bodies. [23]

In Norway, certain species of cyanobacteria produce toxins that can inflict severe liver or nerve damage on animals and humans, potentially leading to paralysis or death. Incidents of livestock mortality have been reported in Norway due to the consumption of water contaminated with high concentrations of toxins from the species Microcystis Aeruginosa. [24]

By reducing the light transmitted through the water, the floating PV panels have the potential to decrease algae growth. This can be useful for lakes with significant algae presence, enhancing water quality and lowering the expenses associated with water treatment. [5]

2.4.4 Reduced water evaporation

Mounting solar panels on top of water reservoirs presents a promising solution for reducing water evaporation and harnessing solar energy simultaneously. This technique has gained attention for its potential to address both energy and water resource challenges, particularly in arid and semi-arid regions where water scarcity is a pressing issue. [5]

A national lake report from 2019 stated that climate change results in both increased precipitation and higher temperatures and that extreme conditions, such as the drought summer of 2018, may become a new normal in a few decades [25].

By covering the water surface with solar panels, evaporation rates can be significantly reduced due to the shade provided by the panels. This shading effect limits direct exposure of the water to sunlight, thereby decreasing the energy available for evaporation. [5]

Furthermore, during nighttime, the solar panels may function as condensing surfaces. As night falls, the panels cool off faster than the water. As water vapor rises from the reservoir, it can come into contact with the cooler surfaces of the solar panels. This contact can facilitate condensation, causing the vapor to return to liquid form, forming water droplets on the panels. This not only benefits water conservation efforts but can also enhance the overall efficiency of solar panel operations. [26]

The presence of water droplets on the solar panel surface can help moderate the rate at which the panel heats up [27]. This can have positive implications for the performance and longevity of the panels, as excessive heat can degrade solar panel efficiency over time. By maintaining lower temperatures, the panels may operate more effectively, thereby maximizing energy output [27].

2.5 Challenges of floating PV in Nordic conditions

There are various challenges when it comes to FPV systems. This section will explore the challenges the FPV installation faces when it comes to solar power being a volatile source; mismatch that occurs due to variations within the PV system; soiling and shading blocking the irradiance; mooring ensuring stability amidst varying weather patterns and water levels; environmental stress leading to degradation of the panels; the operation and maintenance costs associated with FPV systems.

2.5.1 Solar energy as a non-regulatable energy source

The non-regulatable nature of solar energy presents challenges for grid stability and energy planning. Un-

like traditional energy sources such as hydro power or natural gas, where output can be adjusted relatively quickly to match demand fluctuations, solar energy generation is dependent on weather conditions and time of day, making it less controllable.

Solar power variability can introduce instability into the grid, especially when there are rapid changes in generation due to passing clouds or changes in daylight hours. This variability can lead to frequency deviations and voltage fluctuations and can be a challenge for the grid operator as they are obligated to deliver a quality only allowing voltage variations of 10 %. The reason for this regulation of delivery quality is that all electronics are designed to tolerate such fluctuations. If an electronic device is destroyed due to exposure to high voltage, it is the grid operator's responsibility. [28]

This lack of control over solar power requires innovative solutions to ensure reliable and consistent electricity supply, especially during periods of high demand or limited sunlight. A solution to the problem of high voltage in the grid is dynamic throttling of local solar power production. Instead of entirely turning systems off, dynamic throttling can reduce solar production with 10 % and still allow the solar system to operate. [28]

Figure 13 demonstrates the solar production in Norway from January 2021 to December 2023. As well as illustrating how the establishment of new solar panels drastically increased with the energy crisis in 2022-2023, it also demonstrates how production is season-based, resulting in a need for compensation during winter seasons. Utilizing solar energy to pump water back up to reservoirs during the summer season can be a viable strategy for energy storage [29].

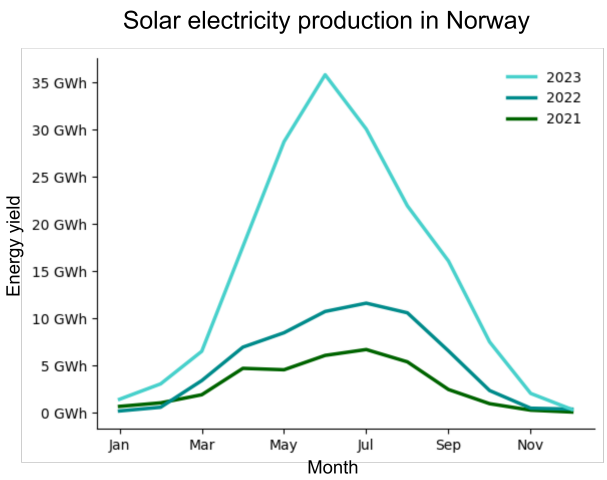

Figure 13: Solar production for Norway, Jan 2021 - Dec 2023. Data source: Elhub [3].

2.5.2 Mismatch

Mismatch losses are a concern in both floating and land-based photovoltaic (PV) systems. These losses stem from variations among modules and disparities in irradiance and temperature distribution across different system locations. Generally, mismatch losses of around 1 percent are considered typical for ground-mounted installations and can be applied to floating photovoltaic (FPV) systems. However, for FPV platforms experiencing significant movement due to waves, misaligned orientations of individual modules may introduce additional mismatch losses. The exact magnitude of these losses depends on various factors, including module tilt, solar position (typically correlated with latitude), the proportion of direct and diffuse light, and wave characteristics. [4]

Quantifying these losses accurately remains challenging, and ongoing research is actively addressing this issue. A simulation study conducted by the Solar Energy Application Centre, a division of the TNO Institute in the Netherlands (TNO-SEAC), suggests potential losses of up to 3% based on observed wave properties in their experimental setup. [4]

2.5.3 Soiling

Soiling losses in photovoltaic systems vary depending on the geographical location, typically falling within the range of 1-3 percent, disregarding sources of soiling such as ice and snow. These losses are influenced by factors such as site conditions and the regularity of cleaning schedules. To effectively reduce soiling-related losses, it is recommended to utilize tilt angles of at least 10°. This inclination facilitates enhanced self-cleaning mechanisms, primarily through natural rainfall, compared to installations with lower tilt angles. [4]

While dust accumulation is less prevalent on water surfaces compared to land, Floating Photovoltaic (FPV) islands have been observed to attract birds,

along with their droppings. Nesting birds are inclined to seek sheltered areas with minimal human interference. The structure of solar panels and the spaces between rows of panels on FPV islands provide such refuge, enabling birds to rest undisturbed. This can lead to significant soiling issues, surpassing the typically assumed 3 percent threshold for soiling. [4]

However, soiling losses across Europe have been shown to be consistently overestimated, as indicated by a recent study [30]. For example, research conducted by the Institute for Energy Technology (IFE) has revealed that during Norway's summer months, typical soiling losses amount to only approximately 0.15%, in contrast to the Norwegian standard suggesting a significantly higher figure of 2% [31].

2.5.4 Shading

Shading is commonly categorized into two main categories: near shading and far shading [32], both of which significantly impact energy yield potential and the selection of suitable installation sites.

Near shading refers to shading caused by objects or structures near the PV system. These objects could be trees, buildings, nearby installations, or even the system's components like inverters or tilted modules. Near shading can lead to decreased energy production as shadows cast over the solar modules obstruct sunlight. [4]

Far shading concerns the topographical features of the surrounding terrain and their potential to obstruct sunlight along the horizon. This can include hills, mountains, or tall structures situated far away from the PV system but still capable of casting shadows that affect energy production. Evaluating far shading losses is crucial during site selection to ensure continuous access to sunlight throughout the day. This is especially important in mountainous regions where terrain features can significantly impact the availability of sunlight. [4]

2.5.5 Mooring

One of the primary challenges of mooring is ensuring the stability and security of the platform amidst varying weather patterns. Strong winds, turbulent waves, and unpredictable currents can exert immense force on the anchoring system, necessitating designs capable of withstanding such pressures. Tilted panels may encounter increased aerodynamic forces depending on wind speed and direction, resulting in increased load on the mooring. [4]

Water depth, water currents, and terrain of the water body play a crucial role in determining the cost of the project and maintenance of anchoring. Having fluctuating water levels complicates the anchoring systems for tilted modules, as they need dynamic designs to ensure that the modules are facing the right direction. [5]

2.5.6 Degradation

FPV systems are exposed to heightened vibration and stress due to the impact of fluctuating temperatures, waves, wind forces, snow, and ice. This extra pressure can make tiny cracks in the panels, causing problems with how long the components last and reducing the panel's efficiency over time. [33]

Additionally, the presence of humidity presents a formidable risk to the operational durability of electrical systems. Notably, saline or brackish coastal environments introduce heightened corrosion susceptibility to metallic components, encompassing structural elements, grounding systems, and electrical connectors and wiring. [4]

2.5.7 Operation and maintenance

Operational and maintenance costs are typically higher for FPV compared to ground-based PV. Accessing PV arrays typically necessitates the use of boats, even when installations feature maintenance pathways. Regular inspection of anchoring and mooring cables is essential, often requiring the expertise of divers. The replacement of parts is also more intricate, demanding adequate safety measures for workers. Additionally, marine environments introduce the challenge of biofouling, making it harder to inspect the anchoring. [5]

2.6 Environmental uncertainty

FPV technology represents a relatively new frontier in renewable energy, and as such, its long-term environmental effects are not yet fully understood. This

section will focus on how the shading and the floating material can affect the aquatic environment.

2.6.1 Shading impacts

The effect of FPV systems on the aquatic environment is an ongoing area of study. A study from 2023 elucidates, for the first time, the shading effects of large-scale FPV power stations on the aquatic environment [34]. Long-term empirical monitoring and data analysis lead to multiple findings.

First being that FPV systems only significantly reduce dissolved oxygen levels in the water directly under them, compared to areas without FPV [34].

Other water quality indicators like chlorophyll, nitrogen, and phosphorus show changes under FPV, but these changes are similar in magnitude to natural variations and don't significantly harm water quality when FPV coverage is less than 50% [34].

FPV has a cooling effect during the day and keeps water warmer at night. This affects peak water temperature, but the changes are gradual and often lag behind areas without FPV [34].

If 10% of the water area larger than 1 km2 in China is utilized for FPV development, it could result in a reduction of over 900 million tons of CO2 emissions and save approximately 5 billion m3 of water. This potential impact is significant in the context of climate change mitigation [34].

A research on how covering fishponds with floating PV affects the fish farm, stated that it is possible to cover up to 60% of the fish pond, while still maintaining more than 70% fish production [35]. They concluded that installing FPV on fishponds may have a moderate negative impact on the fish stock.

2.6.2 Toxin impacts

According to World Bank, floating solar is regarded as environmentally friendly. The floats that uphold the PV panels are typically crafted from a plastic material known as high-density polyethylene (HDPE) [5]. HDPE is a material that is commonly used in drinking water applications, such as pipes, as it is known for its durability and resistance to degradation compared to other types of plastics.

However, prolonged exposure to UV radiation from sunlight can still cause degradation [36]. Some technologies are instead using aluminum as floats, as they are resistant to rust and do not generate microplastics or leach chemicals into the water [9].

There are currently no internationally standardized testing procedures for floats. It is therefore important to evaluate the float quality to reduce the environmental impacts, especially in cases involving drinking water [5].

2.7 Practical constrictions for installing FPV in the near future

There are two primary practical factors influencing the probability of installing floating PV in the near future. The first being grid connectivity, and the second being the availability of the lake. The availability of the lake for FPV deployment is dependent on different factors, two of them being the conservation status of the lake and the risk of flood.

2.7.1 Grid Infrastructure

The expense of connecting a power system to the grid often represents a significant portion of the overall cost. Given the high costs associated with new grid infrastructure, system integrators are frequently advised to position their projects in close proximity to existing grid connections, typically within a range of 1 to 3 kilometers [4]. However, it's important to note the limitations of existing grid capacity, which may constrain the feasibility of new connections.

Floating Photovoltaic (FPV) installations at hydropower plant reservoirs offer a compelling solution to mitigate overall power costs. Sharing the transmission infrastructure enables hydropower to balance the non-regulatable floating PV [14].

2.7.2 Nature conservation

The Norwegian Environment Agency has divided nature preservation into categories: national parks, landscape protection, nature reserves, marine protected areas, and others. National parks are larger areas that show little to no signs of human intervention. Protecting larger areas ensures that the interactions in nature are not disrupted. The landscape-protected areas have a focus on preserving areas with a high ecological, cultural, or experiential value. Nature reserves

represent the most stringent form of area protection. These areas are protected because they possess distinctive scientific value. Marine protected areas can be the seabed, water column, surface, or a combination of these along the Norwegian continental shelf [37].

2.7.3 Flood hazard areas

Flood hazard areas are geographical regions that are prone to flooding due to various factors such as proximity to rivers, lakes, or low-lying topography. There is no standard definition of these flood hazard areas. In Norway, TEK17 describes flood as the inundation resulting from heightened water flow and elevated water levels in rivers, streams, and lakes [38]. Such occurrences may arise from intense precipitation, snowmelt, or damming caused by ice floes or avalanches [38]. Flood hazard areas are identified through flood risk assessments, which consider factors such as historical flood data, topographic maps, hydrological models, and land use patterns [39].

The flood during the extreme weather event "Hans" began with record-high water levels far up in the watercourses, well beyond existing flood zone maps [39]. In the aftermath of the extreme weather event "Hans", insurance companies have been inundated with reports of damage, with approximately 10,000 cases recorded across buildings, properties, and land. Initial estimates from the Norwegian Natural Damage Pool suggest that compensation for these reported damages could reach a staggering 1.8 billion Norwegian kroner. In addition to this, the extreme weather also caused large damage to the infrastructure [40].

Optical and radar-based satellite images were used to map flooded areas, landslides, and debris flows both during and after events like extreme weather events to gain a comprehensive understanding of the situation and plan responses. Satellite data is used to verify and calibrate the hydraulic models underlying flood zone maps [39].

The Sentinel satellites, especially Sentinel-1 for radar imagery and Sentinel-3 for, among other things, measuring snow cover, play a crucial role in NVE's monitoring and warning systems. Image data from these satellites are used not only to map damages and changes during disasters but also to evaluate and improve flood warning systems, as well as to prepare for upcoming events like the annual spring thaw flood [39].

NVE has also developed services and tools based on Copernicus data to analyze changes over time and identify areas that are particularly prone to flooding. This includes the use of detection algorithms to automatically analyze satellite images and identify flooded areas [39].

This integration of satellite data into NVE's work contributes to a better understanding, monitoring, and response to flood crises and other natural disasters, demonstrating the value of space technology in societal safety and environmental monitoring [39].

In accordance with Building Technical Regulations (TEK17), a flood hazard assessment or mapping is required for measures classified as safety class F3 and those falling under § 7-2, first paragraph [41].

2.8 PV efficiency

Standard Test Conditions (STC) serve as the universal standard for testing photovoltaic (PV) modules. These conditions ensure consistency and comparability across different PV modules and systems.

However, the performance of PV systems are dependent on various factors, such as temperature, incidence angle, and system losses. Incorporating these factors into the assessment of PV system efficiency is essential for accurately predicting energy yield in real-world conditions.

This section will describe how utilizing temperature models and incidence angle modifiers, along with accounting for system losses, gives a more realistic prognosis of the energy potential, starting by describing the standard test conditions in more detail.

2.8.1 Standard test conditions - STC

Solar cells and photovoltaic modules are manufactured by various companies and research laboratories, and there is a wide range of solar cell technologies available in the market. The standard test conditions (STC) have been established to enable fair comparisons among different PV modules. The STC is defined by specific parameters, including an irradiance of $1000\,\mathrm{W/m^2}$, an AM1.5 spectrum, and a cell temperature of $25\,^{\circ}\mathrm{C}$.

The AM1.5 spectrum, outlined in the International Standard IEC 60904-3, serves as a reference solar spectral distribution. This spectrum is based on the solar irradiance received on a Sun-facing plane surface tilted at 37° to the horizontal. It considers direct sunlight, diffuse sunlight, and the wavelength-dependent albedo of light bare soil. Albedo represents the portion of solar radiation reflected by the Earth's surface and varies based on the environment's reflectivity. The total irradiance of the AM1.5 spectrum is $1000\,\mathrm{W/m^2}$, which closely approximates the maximum solar radiation received at the Earth's surface on a cloudless day.

2.8.2 Temperature-dependent efficiency

The temperature-dependent efficiency, denoted as η_T, can be expressed as a function of the module temperature:

$$\eta_T = \eta_{nom} \times [1 - \beta(T_{mod} - T_{STC})], \tag{2}$$

where η_{nom} is the nominal efficiency measured at standard test conditions (STC), with a temperature of 25 °C, global plane of array irradiance of 1000 $\frac{\mathrm{W}}{\mathrm{m^2}}$. The parameter β is the temperature coefficient, indicating the material-dependent rate of change of efficiency with temperature [42].

2.8.3 Thermal model

Various models have been developed to assess and estimate the temperature of PV modules under different conditions. A study done by Faiman, determined that a modified version of the Hottel–Whillier–Bliss (HWB) equation, originally designed for the analysis of flat-plate solar-thermal collectors, can predict module temperatures with an accuracy comparable to the typical temperature differences observed between individual cells within a module [43]:

$$T_{mod} = T_{amb} + \frac{G_{POA}}{U_0 + U_1 \times v}, \tag{3}$$

where T_{mod} is the PV module temperature that is related to the ambient temperature, T_{amb}, the plane of array irradiance, G_{POA}, the constant heat transfer component, U_0, and the convective heat transfer components U_1.

The practical application of U_1 is frequently hindered by the challenge of obtaining precise wind speed measurements that accurately represent the specific height and positioning of the modules. This difficulty often arises due to the complexities involved in acquiring such measurements. Consequently, a single U-value is often derived, lacking explicit consideration of wind dependency and instead implicitly assuming an average wind velocity [14]:

$$T_{mod} = T_{amb} + \frac{G_{POA}}{U}. \tag{4}$$

2.8.4 Incidence angle modifier - IAM

Standard Test Conditions (STC) measurements involve positioning the photovoltaic (PV) device perpendicularly to the light source. However, in real-world scenarios without dual-axis tracking, sunlight hitting a PV module rarely arrives at such an ideal angle. Instead, it comes in at varying incidence angles ($\theta_i \neq 0°$) throughout the year [44].

To address losses resulting from increased incidence angles, an incidence angle modifier, IAM, is introduced. The ASHRAE IAM model is an incidence angle modifier developed by Souka and Safat (1966), and is commonly used to represent the impact that the angle of incidence has on the performance of PV modules [45]:

$$IAM = 1 - b_0(\frac{1}{cos\theta_i} - 1), \tag{5}$$

in which θ_i is the incident angle, and the b_0 is a parameter used to adjust the IAM model and has a typical value of 0.05. The ASHRAE IAM model has its advantages by having only one parameter b_0, but by having a discontinuity for 90 degrees it has low accuracy for incident angles from 80° to 90° [45].

As illustrated in Figure 14, the optical losses increase rapidly for AOI > 50°. The angular dependent losses are primarily due to the increase in reflection at the glass-air interface but also include the increase in absorption in the front materials as the distance traveled through the front glass increases with increased angle of refraction [44]. The IAM factor provides a way to adjust the nominal efficiency, with respect to that AOI of 0°, the solar refracted radiation intensity based on the angle at which the sunlight strikes a surface.

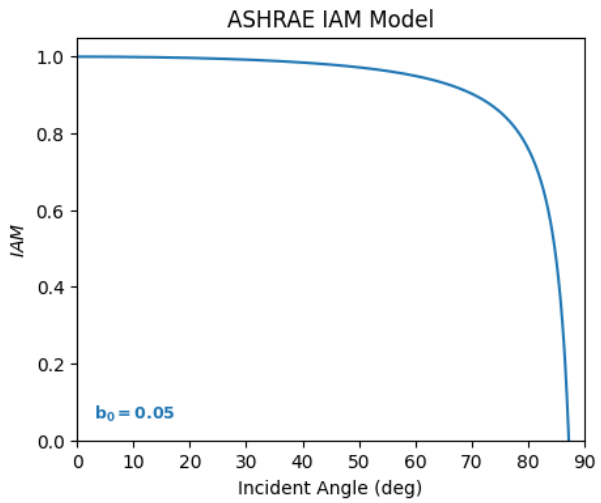

Figure 14: The ASHRAE incident angle modifier (IAM) model from Eq.5 illustrates how an increased incident angle reduces the refracted light onto the PV module.

The modified module efficiency η_{mod} can be represented as:

$$\eta_{mod} = \eta_T \times IAM. \tag{6}$$

2.8.5 System efficiency

Considering the entire system, various factors contribute to system losses. The following factors contribute to the overall derate of efficiency of a solar power system:

- **LID (Light-induced Degradation):** Exposure to sunlight can decrease the efficiency of a solar cell by 2–3% within the initial weeks of installation.
- **DC cabling:** Losses associated with the direct current (DC) wiring.
- **Diodes and connections:** Losses incurred due to diodes and interconnections within the system.
- **Inverter:** Conversion losses as the inverter transforms DC generated by solar panels into usable alternating current (AC) for grid integration.
- **Transformers:** Efficiency losses in voltage transformation processes before grid delivery.
- **AC wiring:** Losses occurring in the alternating current (AC) wiring connecting the inverter to the electrical grid or load.
- **Shading:** Refers to the impact of nearby objects casting shade on the solar panels.
- **Soiling:** Losses due to accumulation of particles, reducing the efficiency by blocking sunlight from reaching the photovoltaic cells.
- **Mismatch:** This term typically refers to losses caused by mismatches in components within the solar energy system, such as modules or inverters.
- **Availability:** Percentage of system loss attributed to inverter downtime.

The overall system efficiency η_{sys} can be expressed as:

$$\eta_{\text{sys}} = \eta_{\text{mod}} \times \prod_{i=1}^{N} D_i, \tag{7}$$

where $\Pi_i^N D_i$ is the product of all derate factors. By applying equation 2-7, the nominal efficiency can be adjusted to reflect more realistic values for each specific location.

The power output of the photovoltaic system can be calculated using the following equation:

$$P = \eta_{sys} \times A \times G_{POA}, \tag{8}$$

3 Methodology

This chapter presents the research methodologies utilized to evaluate the potential energy yield of floating photovoltaic (FPV) systems in Norway. Before delving into the specifics of the data utilized and the resolution of the research questions, a general overview of the methods employed will be provided to establish a foundational understanding of the process.

3.1 Process description

This research aims to find the potential energy yield of floating photovoltaic (FPV) in Norway, with a focus on local energy generation. Five distinct scenarios were investigated:

1. **Maximum Coverage Scenario:** This scenario estimates the energy yield by covering 100% of all lakes in Norway, referred to as roof production. This approach helps identify the maximum potential energy yield without any constraints.
    - *Rationale:* Understanding the upper limit of FPV potential provides a benchmark for evaluating more realistic scenarios. It helps gauge the theoretical maximum capacity of FPV systems if no restrictions were applied.
2. **Socially Accepted Potential:** To meet municipal approval requirements, projects must avoid nature-reserved areas and flood hazard zones. Excluding these areas ensures more accurate and socially acceptable results. This scenario limits the coverage to 10 % of lake surfaces, reflecting societal and environmental constraints.
    - *Rationale:* Limiting coverage to 10 % aligns with common practices in broader studies, ensuring the deployment is environmentally sustainable and socially acceptable. This constraint also aligns with previous research for combining hydro plants with solar plants in Europe [29].
3. **Local Energy Potential:** This scenario filters out lakes without a substation within 2 km, providing an indicator of the potential for local energy production. The 2 km constraint aligns with the World Bank Group's guidelines for optimal local production sites, ensuring feasible and cost-effective grid connectivity.
    - *Rationale:* Proximity to substations reduces transmission losses and infrastructure costs, making FPV deployment more viable and cost-effective. This constraint ensures the selected sites are practical for local energy generation.
4. **Contribution to 8 TWh Target:** This scenario assesses the extent to which local FPV deployment can contribute to the 8 TW h target by 2030, leveraging the Norwegian Water Resources and Energy Directorate's (NVE) recommendation of a 5 MW threshold for concession requirements. Each substation can only connect to one FPV system, and the land-based connection point must be within a 2 km radius of the substation.
    - *Rationale:* Evaluating the practical feasibility of FPV systems in meeting national energy goals helps in understanding their potential role in achieving the 8 TW h target. The 5 MW threshold facilitates quicker approvals and installations, supporting rapid deployment.
5. **Hydro Plant Combination:** This scenario explores the potential of combining hydro plants with FPV systems, with constraints of covering a maximum of 25 % of the reservoir area and not exceeding the hydro plant's installed capacity.
    - *Rationale:* Combining FPV systems with existing hydro plants leverages existing infrastructure, enhancing renewable energy generation without significant additional costs. The 25 % coverage constraint ensures minimal impact on the reservoir's primary functions.

Estimating the energy yield potential for the five scenarios involves multiple phases: initially; identifying areas for deployment based on geospatial data analysis; estimating the potential energy yield based on meteorological data from the selected center points and scaling it up to the selected areas. Lastly, the distribution of energy yield potential across spot price

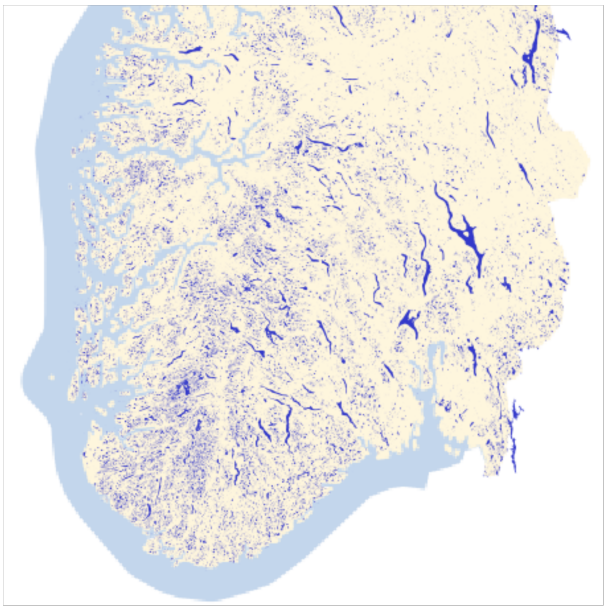

Figure 15: Map over lakes in Norway. Full map is provided in Appendix A Figure 34. Source: [46]

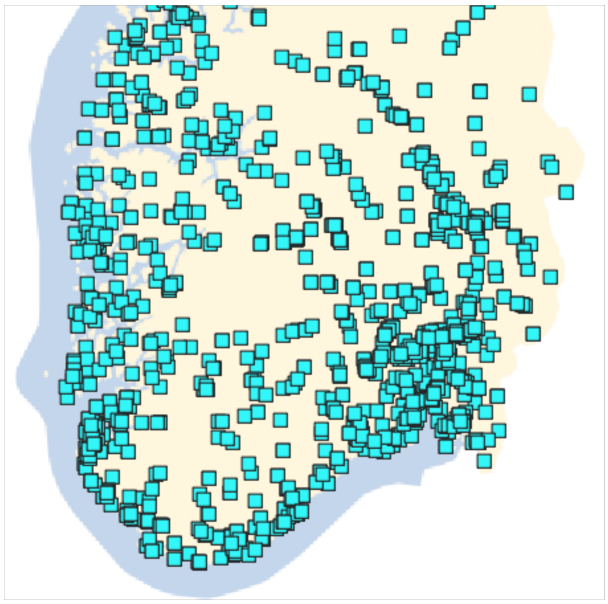

Figure 16: Map of Norwegian substations. Full map is provided in Appendix A Figure 37. Source: [46]

regions will be found for scenario 4 and 5, as well as the top 10 municipalities with highest potential.

This methodology seeks to not only understand the total potential energy yield but also the portion that can be realistically harnessed in the near future without requiring extensive investments in infrastructure.

3.2 Data Description

Geospatial data was acquired from several sources. The primary source of geospatial data was the Norwegian Water Resources and Energy Directorate (NVE), providing information on lakes, substations, and flood hazard areas. Data on nature-reserved areas and municipality regions were obtained from the Norwegian Environment Agency.

Utilizing PVGIS API version 2, typical meteorological years were gathered from PVGIS-SARAH2 and PVGIS-ERA5 solar radiation data. Meteorological parameters such as temperature at 2 meters and global irradiance were collected from PVGIS, while the solar position data was sourced from the pvlib Python package.

3.2.1 Geospatial data

The NVEs lake database is developed based on N50 map data and updated once a year [47]. The N50 map data belongs to the Norwegian Mapping Authority and is cartographically edited according to presentation rules equivalent to the main map series Norway 1:50,000 [48], [49]. The data is not complete, and duplicates may occur [47].

The substation database is part of the grid system dataset in the public map foundation (DOK), consisting of public geographic data tailored for municipal planning and building permit processes and is updated two times a year [46], [50], [51]. The data was collected between 2010 and 2018. Some areas may have been updated after 2018. The location is often not precise and deviations of several tens of meters may occur [52].

NVE's flood hazard map is a national dataset showing areas prone to flooding. It's tailored for municipal use, serving as an initial assessment tool for impact evaluations and risk analyses related to municipal plans. In accordance with Building Technical Regulations (TEK17), a flood hazard assessment or mapping is required for measures classified as safety class F3 and those falling under § 7-2, first paragraph. [41]

Data on conserved areas were obtained from the Norwegian Environment Agency. This dataset provides an overview of areas protected under the following legislation [54]:

- Nature Diversity Act of 2009

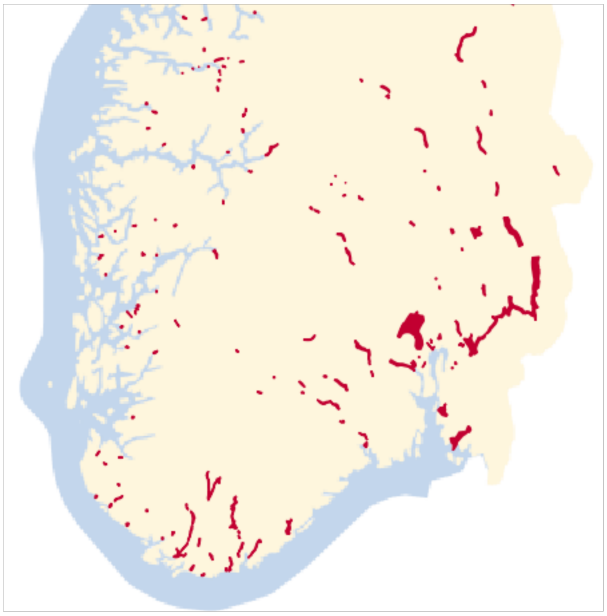

Figure 17: Flood hazard areas in Norway. Full map is provided in Appendix A Figure 36. Source: NVE (data) [46], The Norwegian Mapping Authority (background) [53].

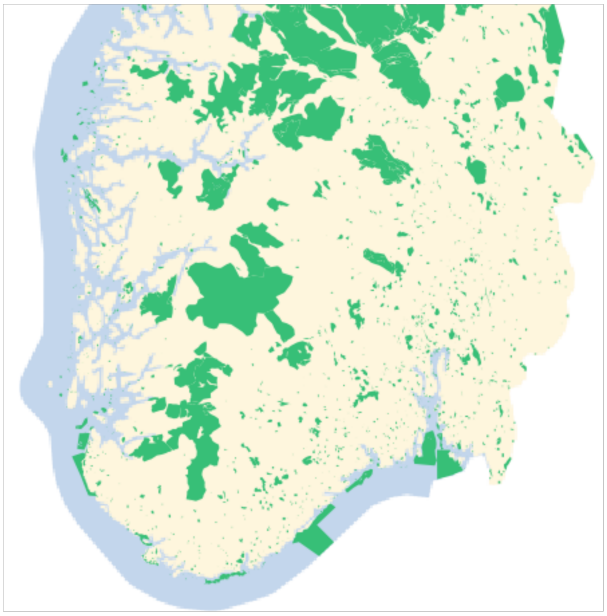

Figure 18: Nature-conserved areas in Norway. SFull map is provided in Appendix A Figure 35. Source: NVE (data) [46], The Norwegian Mapping Authority (background) [53].

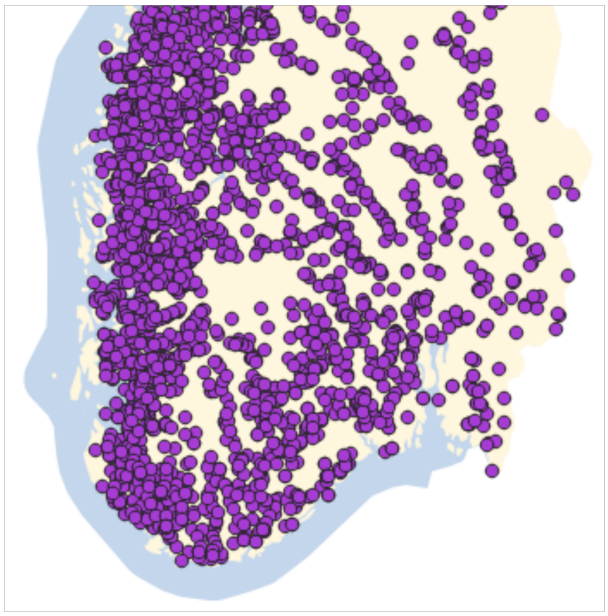

Figure 19: Map of Norwegian hydropower plants. Full map is provided in Appendix A Figure 39. Source: NVE (data) [46], The Norwegian Mapping Authority (background) [53].

- Svalbard Environmental Act of 2002.
- Biotope protection under the Wildlife Act of 1981
- Nature Conservation Act of 1970
- Nature Conservation Act of 1954
- Jan Mayen act of 1930
- Svalbard Act of 1925
- Nature Conservation Act of 1910.

The precision of the maps may vary with older establishment dates.

The hydropower station datset (Figure 19) and the regulated reservoirs (Figure 20) were obtaiend from NVE. The dataset includes all reservoirs and regulated lakes regardless of their purpose. The specification covers both operational and non-operational facilities. [55]

NVE's market balancing areas, illustrated in Figure 21, represent regions within Norway where electricity spot prices are uniform. Variations in electricity spot prices may occur due to factors such as demand-supply dynamics and transmission constraints between the areas [56].

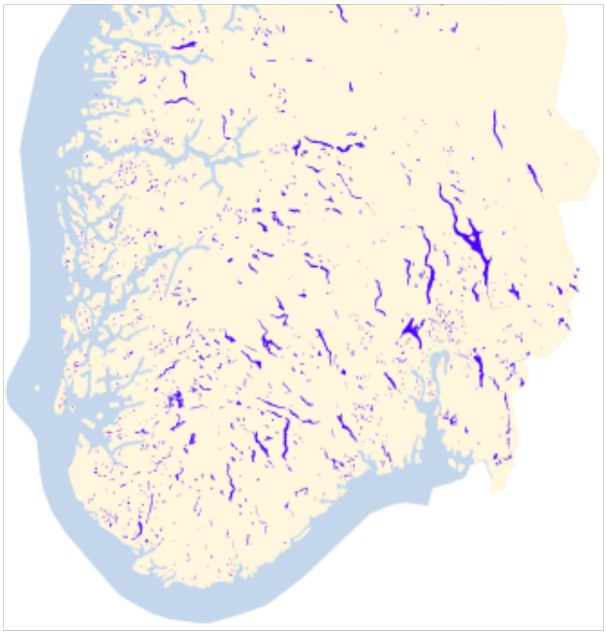

Figure 20: Map of regulated reservoirs in Norway. Full map is provided in Appendix A Figure 38. Source: NVE (data) [46], The Norwegian Mapping Authority (background) [53].

Figure 21: Map of Norwegian market balancing areas. Source: NVE (data) [46], The Norwegian Mapping Authority (background) [53].

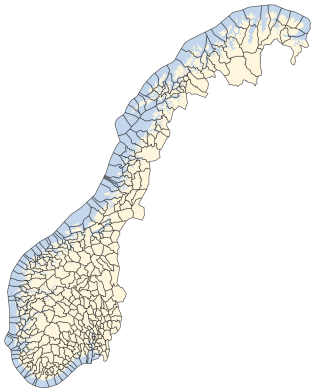

Figure 22: Map of Norwegian municipalities. Source: The Norwegian Mapping Authority [53], [57].

The dataset of Norwegian municipalities (Figure 22) belongs to the Norwegian Mapping Authority and contain 357 municipalities.

3.2.2 Weather Data Models: PVGIS-ERA5 and PVGIS-SARAH2

PVGIS (Photovoltaic Geographical Information System) is an invaluable tool developed by the European Commission's Joint Research Centre (JRC) for assessing solar energy potential. This system leverages various databases to provide accurate and reliable solar radiation and meteorological data. Two key datasets offered by PVGIS are PVGIS-ERA5 and PVGIS-SARAH2, each with distinct characteristics and applications. [58]

PVGIS-ERA5 is based on the fifth generation of the European Centre for Medium-range Weather Forecasts (ECMWF) reanalysis dataset. Reanalysis is a method used in meteorology to create comprehensive datasets of past climate conditions. It involves assimilating historical observational data from various sources (such as satellite observations and ground-based observations) into a consistent global atmospheric model. This process generates datasets that can be used for climate monitoring, research, and assessment. [59]

- **Spatial Resolution**: $0.25° \times 0.25°$ (ca. 31 km).
- **Temporal Coverage**: From 1940 to the present.
- **Type**: Reanalysis dataset.
- **Data Frequency**: Hourly.

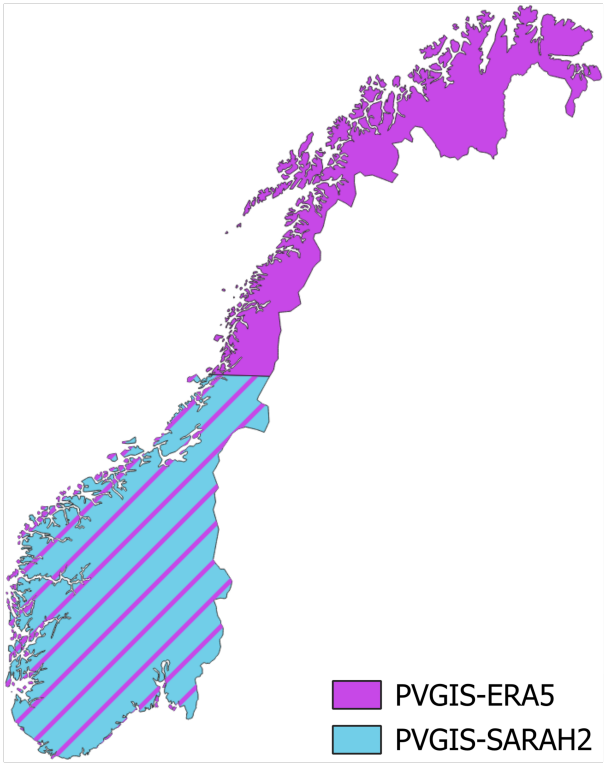

Figure 23: PVGIS solar radiation coverage area for Norway. PVGIS-SARAH2 has only data up to 65° latitude, where as PVGIS-ERA5 has full coverage of Norway.

The extensive temporal coverage and high frequency of data make PVGIS-ERA5 particularly useful for analyzing historical climate patterns and assessing long-term trends in solar energy resources. Its broader spatial resolution ensures comprehensive geographic coverage, including regions beyond the latitude 65° N, which encompasses the northern parts of Norway. However, because latitudes above 65° N are not covered by geostationary satellites and ground-based observations are sparse in northern Norway, the accuracy of the ERA dataset is lower in these northern regions [60].

PVGIS-SARAH2 is derived from the Satellite Application Facility on Climate Monitoring's (CM SAF) Surface Solar Radiation Data Set - Heliosat (SARAH-2). This dataset utilizes satellite observations from the MVIRI and SEVIRI instruments aboard Meteosat satellites, providing high-resolution data for solar energy assessment. [61]

- **Spatial Resolution**: 0.05°×0.05° (ca. 5.5 km).
- **Temporal Coverage**: From 1983 to 2015.
- **Type**: Satellite-derived climate dataset.
- **Data Frequency**: Hourly.

The higher spatial resolution of PVGIS-SARAH2 allows for more detailed and precise assessments of solar radiation, making it ideal for localized solar energy projects and site-specific evaluations. However, its geographic coverage is limited to latitudes below 65° N, excluding the northernmost parts of Norway.

Comparative Analysis

A study conducted by IFE (Institute for Energy Technology) demonstrated the superior performance of PVGIS-SARAH2 in various regions within Norway's lower latitudes. The study compared the accuracy of solar radiation estimates from different datasets, including PVGIS-SARAH2 and PVGIS-ERA5, by evaluating their relative mean absolute error (rMAE) and relative mean bias error (rMBE) [60]. The results showed notable differences between the two datasets:

- **PVGIS-ERA5**:
  - Median rMAE: 27.1%
  - Median rMBE: 5.2%
- **PVGIS-SARAH2**:
  - Median rMAE: 20.3%
  - Median rMBE: -0.1%

The findings indicates that PVGIS-SARAH2 consistently provided lower rMAE values, indicating higher accuracy in the estimation of solar radiation. Additionally, the rMBE for PVGIS-SARAH2 reflected minimal bias. In contrast, PVGIS-ERA5 had higher rMAE and a positive rMBE, indicating that it tended to overestimate solar radiation.

Despite the geographic limitations of PVGIS-SARAH2, its higher resolution and improved accuracy make it a valuable tool for solar energy assessments in the covered regions. The precise data from PVGIS-SARAH2 helps improving the performance of the energy yield assessment.

3.3 Area selection

In the assessment of energy yield potential, finding realistic area measurements for installing floating PV is essential to ensure a qualified prediction within an acceptable range of uncertainty. This section outlines the methodology employed to determine the gross area, the socially accepted areas, the practical available area, and the hydro plant reservoir area used during the energy yield assessment.

3.3.1 Gross and social accepted area

A flowchart describing the process of selecting the gross (scenario 1) and socially accepted areas (scenario 2 and 3) can be viewed in Figure 25. The gross area, which served as the basis for estimating roof production, was calculated as the sum of all lake areas. To determine the socially accepted area, any lake arrays falling within a designated reserved or flood hazard area were excluded from the dataset. Subsequently, the resulting area underwent adjustment to ensure it did not surpass 10% of the total lake area.

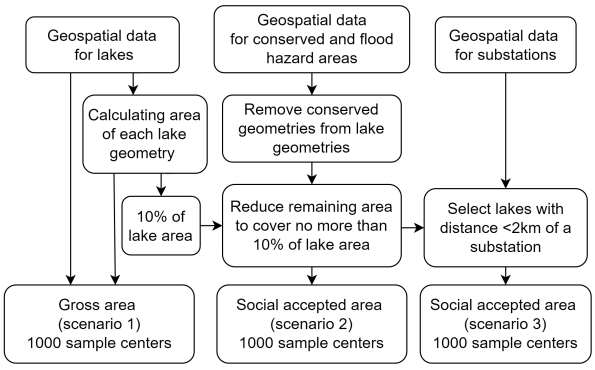

Figure 24: Flowchart for area selection of scenario 1-3.

3.3.2 Practical area selection

The process of selecting the practical area began by identifying coastlines within 2 km from a substation (Figure 26b). The distance of 2 km was chosen based on the recommended distance to grid connectivity being 1-3 km [4]. From there, the lake surface between 20 m and 300 m from the coastline was chosen (Figure 26c). The distance of 300 m was roughly calculated from having a yearly peak irradiance at 700 W/m^2. To get a power output of 5 MW, assuming an efficiency of

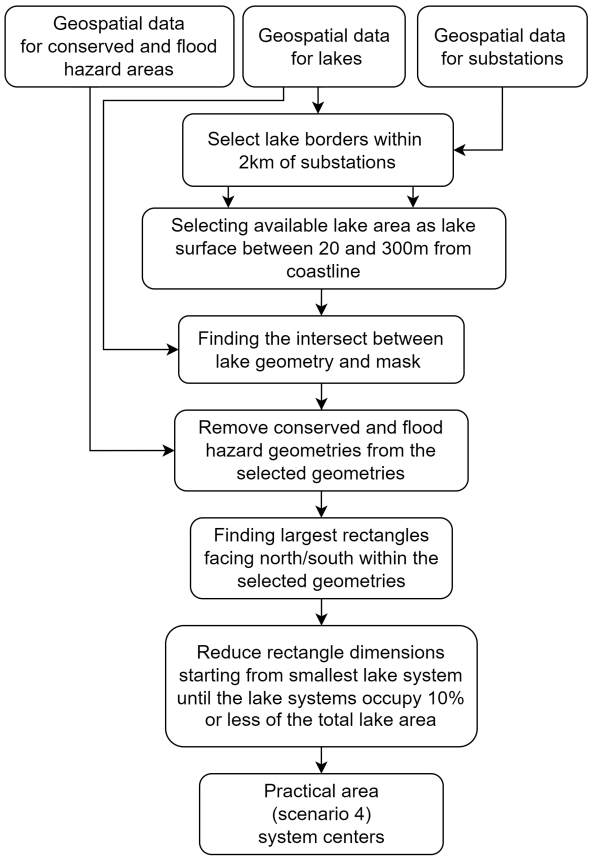

Figure 25: Flowchart for area selection of scenario 4.

approximately 16 %, you would need a system area of $210 \times 210\,m^2$. As the systems don't have to be square shaped, the distance was rounded up to 300 m.

The next step was to remove restricted and flood-hazard areas (Figure 26d). In cases where selected areas overlapped due to multiple substations in the vicinity, the largest one was selected (Figure 26e). Then, the largest rectangles within the selected areas were selected (Figure 26f). As some substations had multiple lakes within 2 km distance, only the largest system was selected with the purpose of not overloading the substation. In order to maintain lake coverage within the desired limit of 10%, the system areas were reduced in ascending order until the total system area for each lake matched or fell below 10% of the lake's surface.

3.3.3 Faults within practical area selection

As illustrated in figure 27, the method used for finding the practical area identifies the largest rectangle where

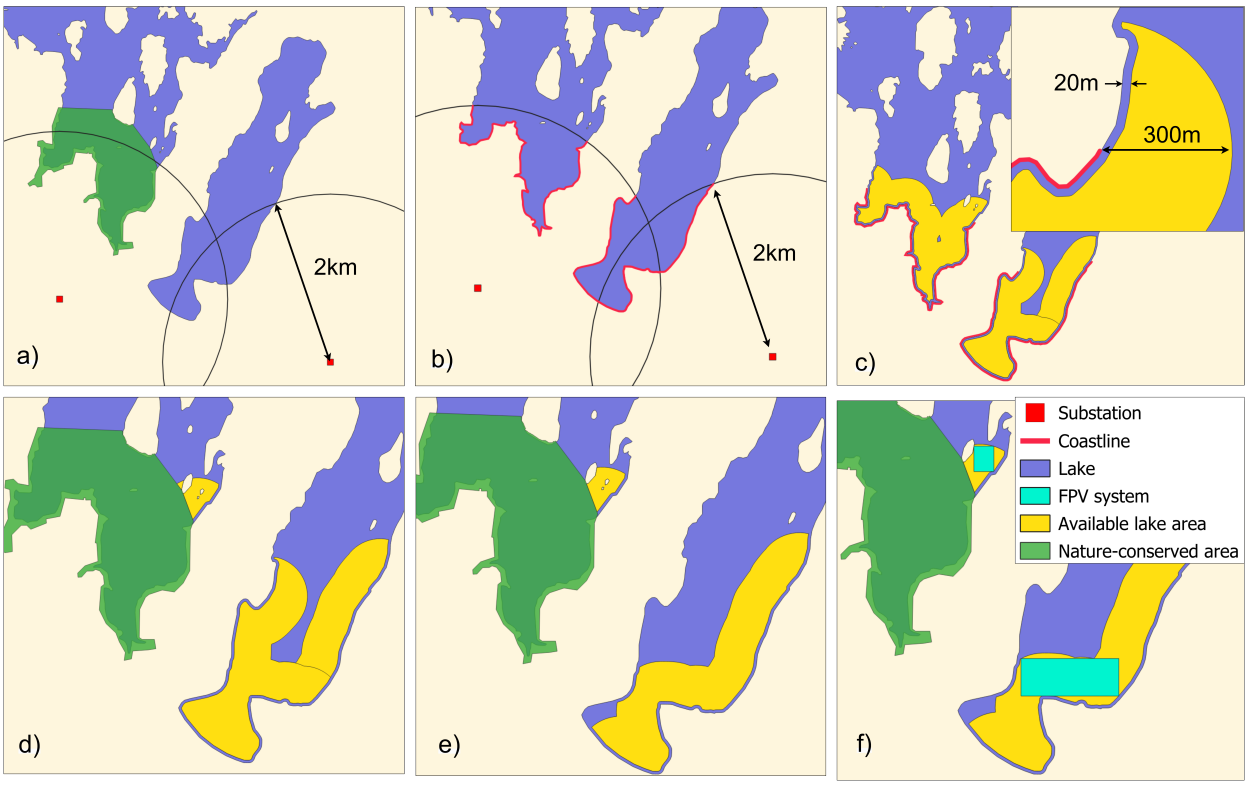

Figure 26: The process of selecting the practical area began by identifying coastlines within 2km of a substation (Fig. a+b). The available lake area was defined as the surface between 20m and 300m from the coastline (Fig. c). Following this, the restricted and flood-hazard areas were excluded (Fig. d). In cases where available lake areas overlapped due to multiple substations in proximity, the largest polygon was selected (Fig. e). Next, the largest rectangles within the available lake area were found (Fig. f). Each substation was then limited to having only one FPV system. To adhere to the prescribed limit of 10% lake coverage, the size of FPV systems was progressively reduced until the total system area for each lake met or fell below 10%.

all sides of the rectangle remain within the specified array. Islands and areas of water situated more than 300 m from the coastline can be found within these rectangles.

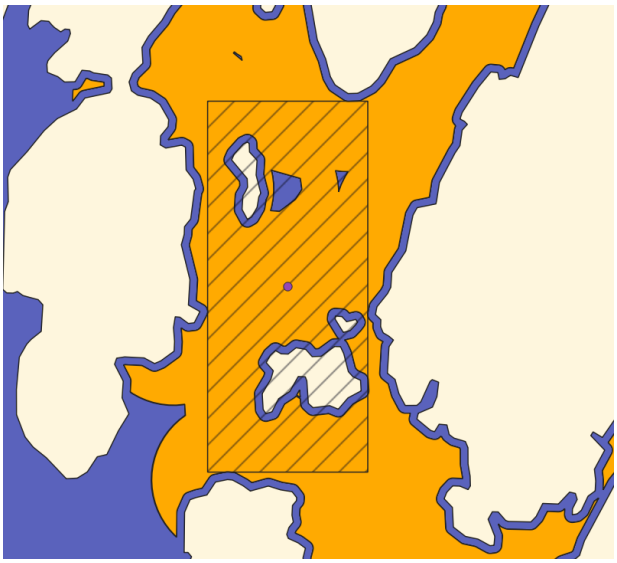

Figure 27: Demonstration of how the largest rectangle within the selected area does not care if there are islands within the system, as long as the edges are covered.

3.3.4 Hydro plant reservoir area

The selected areas for hydro reservoirs were compiled by merging information on hydroelectric power plants and reservoirs, using the power plant names as the primary identifier. This consolidation aimed to obtain the maximum capacity of the hydro reservoirs. In cases where a power plant name corresponded to multiple results for both hydropower and reservoirs, the capacities and areas were aggregated.

To select reference points for gathering weather data, the center of each reservoir was chosen. For practicality, the selected area for weather data collection was set at 25% of the reservoir area, similar to what was done in research for combining hydro plants with solar plants in Europe [29].

Due to that some hydroelectric power plant names had multiple results for both hydropower and reservoirs, the capacity and area were aggregated. In instances where aggregation was necessary for hydro plants, the center of the first sample was chosen as the reference point. This approach was favored over calculating a mean center, as the latter was deemed impractical due to variations in resolution among datasets. For instance, while the horizon dataset has a high resolution of 90 meters, the solar radiation grid offered a lower resolution of either 5 or 25 km, depending on location. The assumption was that the horizon's resolution would significantly impact the assessment, and the center of individual lakes were more likely to share similar horizon characteristics, compared to the mean center.

3.4 Energy yield estimation

This section will start with a general overall description of the energy yield estimation of the gross, socially accepted, practical, and hydro reservoir area, before diving deeper into how the calculation of energy yield was done and what PV module parameters and system losses were used during the calculation.

3.4.1 Energy yield estimation process

This section describes the process of estimating the energy yield potential for the four scenarios, illustrated as a flowchart in Figure 28.

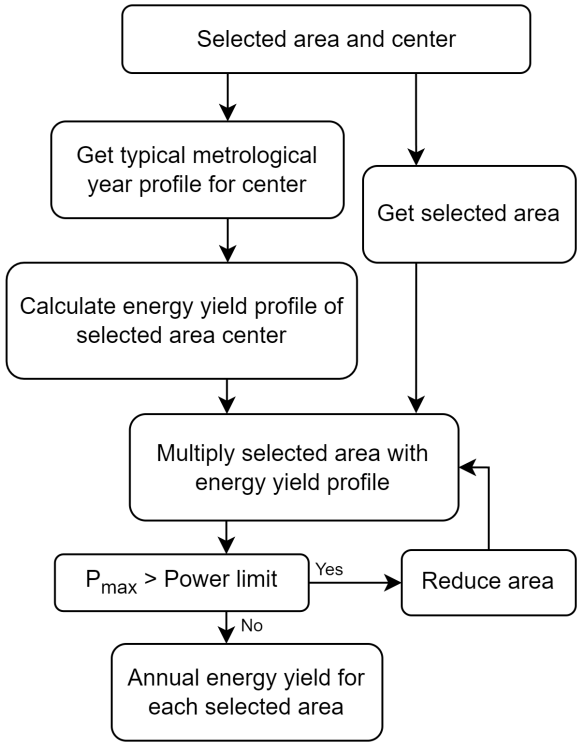

Figure 28: Flowchart for energy yield estimation of a PV array

Initially, the power profile was computed for the

selected area centers, then multiplied by the selected area to determine the total power output. Where power profiles exceeded the power constraint, the respective area was scaled down so that the maximum power output aligned with the power limit. As presented in Table 1, the roof production and the social accepted potential had no upper power limit. However, the practical potential adheres to NVE's suggestion of a 5 MW limitation for local power production, thereby eliminating the need for concession applications [2].

Table 1: Power limits for the selected scenarios investigated in this report.

Scenario	Power limit
Roof production	None
Social accepted potential	None
Social accepted within 2km	None
Practical potential	5 MW
Hybrid with hydro	Max capacity of hydro plant

Annual and monthly production was determined by aggregating the power output times an hour given that the power output was based on meteorological model with an hourly resolution.

Given the dataset's size, containing 267 194 lake geometries, individually estimating energy for each lake would be computationally expensive. Instead, a randomized selection of 1,000 sample centers were chosen for estimating an average annual energy yield per square meter, and then scaled up to the gross and socially acceptable area.

3.4.2 Calculating power profile of system center

The PVGIS API version 5.2 was employed to retrieve typical meteorological data, encompassing global irradiance, surface temperature measured at a height of 2 meters above the surface, originating from the selected centers. In regions where PVGIS-SARAH2 did not provide coverage, PVGIS-ERA5 served as an alternative source of data. Table 2 lists the parameters used for estimating the energy yield.

* From Sunlit Sea data sheet [9]

** From IFE research [14]

The temperature-dependent efficiency, η_T, was calculated from Eq. 2. The temperature coefficient β was set to $0.004\,\mathrm{K}^{-1}$, the same as for the sunlit sea product [9]. The temperature profile of the models was calculated using Eq. 4, with a U-value of $46\,\mathrm{W/m^2K}$. The U-value was found by a research on cooling of floating photovoltaic, for a steady state conditions with only clear sky period using air-cooled string and the ambient air temperature [14].

Table 2: PV module parameters for estimating the power profiles.

Term	Value	Unit
$tilt$	0	deg
$eff_{nom}{}^{*}$	19	%
U^{**}	46	W/m^2K
β^{*}	0.004	K^{-1}

To account for the effect of incident angle on efficiency, an incident angle modifier was calculated from Eq. 5 adjusting the temperature-dependent efficiency to get the module efficiency, η_{mod}, with Eq. 6. This adjustment ensures that higher incident angles, which reflect more rays off the surface, are appropriately considered. The incident angle was computed utilizing the pvlib Python package.

The overall system efficiency was calculated from Eq. 7, with the derate factors in Table 4. The derate factor from soiling loss was time and location dependent for this simulation. The guided soiling loss from Norwegian standard, NS 3031 (Table 3) of the closest municipality center (Appendix B) was utilized to find the derate soiling factor. The cities with their respective center points is listed in Table 9.

The power profile of the system centers were calculated from Eq. 8, with the area being the respective system areas of the system centers. As the weather data had an hourly resolution, the energy yield was calculated by multiply the power profile with an hour.

3.5 Area selection and PV simulation in Python

The area selection is extracted by utilizing the python package geopandas, and visualized in QGIS. The simulation framework is built upon the Python programming language, utilizing classes structure to represent key components such as PV models, PV systems, Lakes, and the overall FPV simulation. Lastly the energy yield at each lake or system is mapped in 3D bar map in excel. The repository is available at: GitHub.

Table 3: Guiding percentage loss due to soiling, from Norwegian Standard: NS 3031

Municipality	Jan	Feb	Mar	Apr	May	Jun	Jul	Aug	Sep	Oct	Nov	Des
Stavanger	15	15	2	2	2	2	2	2	2	2	2	15
Oslo	60	75	60	2	2	2	2	2	2	2	15	45
Trondheim	60	75	45	8	2	2	2	2	2	2	15	54
Tromsø	75	75	75	75	2	2	2	2	2	30	45	60
Bergen	15	30	15	2	2	2	2	2	2	2	2	23
Kristiansand	45	75	45	2	2	2	2	2	2	2	2	38
Lillehammer	75	75	75	30	2	2	2	2	2	2	30	75
Drammen	75	75	60	8	2	2	2	2	2	2	15	53
Skien	75	75	60	8	2	2	2	2	2	2	15	53
Tønsberg	45	75	60	8	2	2	2	2	2	2	8	38
Fredrikstad	15	30	15	8	2	2	2	2	2	2	2	8

3.6 Implementation of AI

Artificial intelligence (AI) has played a supporting role in every aspect of the project. ChatGPT 3.5 has been implemented primarily to enhance language capabilities and debug code. Additionally, ChatGPT has acted as a valuable sparring partner, providing valuable insights and refinement throughout the process.

Table 4: Derate factors utilized during energy yield assessment.

Item	Typical
LID*	0.98
DC cabling*	0.98
Diodes and connections*	0.995
Inverter*	0.96
Transformers*	0.97
AC wiring*	0.99
Shading*	1
Availability of system*	0.98
Mismatch**	0.97
Soiling	1 - soiling loss (Table 3)
Overall at STC	0.837

* Derate factors based on measured losses and component specifications from 24 PowerLight PV systems (twenty single-crystalline silicon, two multicrystalline silicon, and two amorphous silicon) located throughout the United States [62].
** Missmatch suggested by the Solar Energy Application Centre based on observed wave properties in their experimental setup.

4 Results

This section presents the findings derived from the examination of Norwegian lake areas and the estimation of energy yield potential of FPV deployment. Five scenarios have been investigated to address the research question:

1. Roof production: 100% lake coverage
2. Social acceptance: 10% lake coverage, while not covering conserved or flood hazard areas.
3. Local social acceptance: 10% coverage of lakes within grid connection within 2km distance, while not covering conserved or flood hazard areas.
4. Practical: Each substation, located within a 2km radius, is limited to hosting an FPV system with a maximum capacity of 5MW. Furthermore, systems are restricted to occupying no more than 10% and not to cover conserved or flood hazard areas of the lake surface to ensure environmental preservation.
5. Hydro: Exclusively FPV deployment on hydro plant reservoirs, with limitations of not exceeding the maximum capacity of the hydro plant or covering more than 25% of the reservoir surface.

Initially, an overview of the results will be provided, followed by a breakdown of scenario 4 and 5 into regional aggregations concerning municipalities and price zones.

4.1 Overview of results

Table 5 provides an overview of the total energy yield estimated for scenario 1-5.

Table 5: Estimated energy yield for scenario 1-5.

Scenario	Energy yield potential
1	1970 TWh/year
2	171 TWh/year
3	30.9 TWh/year
4	2.6 TWh/year
5	20.4 TWh/year

This study found that Norway has a total lake area of 18 600 km^2, based on the 267 193 lake geometries provided by NVE. Covering 100 % of these lake surfaces with FPV cells has the potential to produce 1970 TWh/year and represents the roof production in this report.

In contrast, scenarios 2 and 3 reflect a more realistic approach by restricting FPV deployment to 10% of lake areas while avoiding conserved or flood hazard zones. Despite the reduced coverage, these scenarios demonstrate substantial energy yield potentials

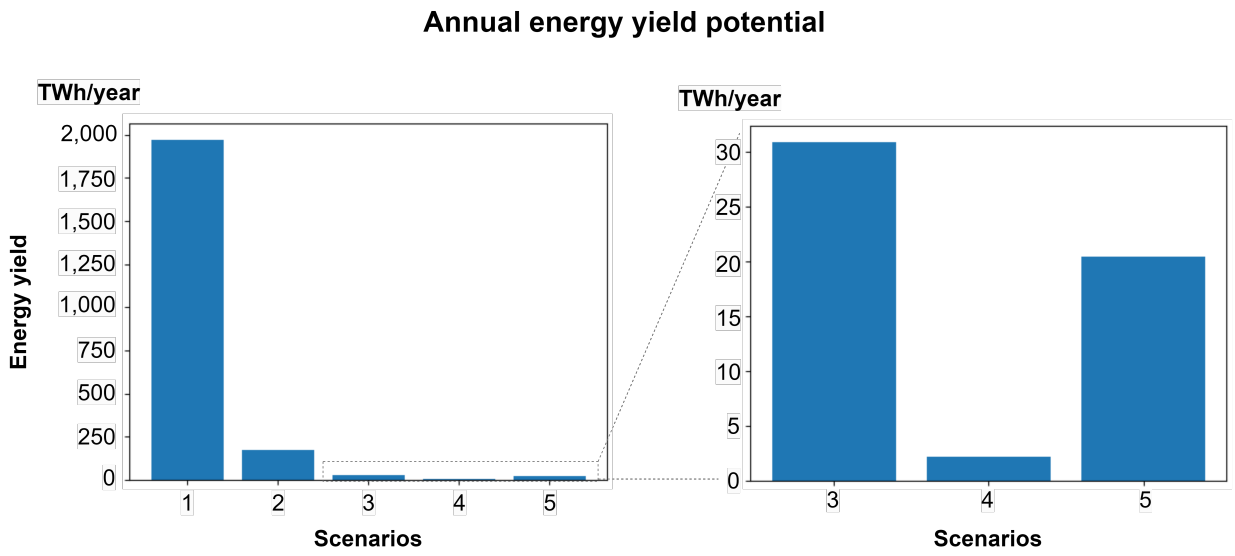

Figure 29: Overview of the results for the five scenarios.

of 171 TWh and 30.9 TWh, respectively. Notably, the constraints applied in scenario 3 to ensure grid connectivity within a 2 km distance resulted in the identification of 5250 viable lakes, as illustrated in Figure 30. These lakes were primarily situated around coastal regions, with clusters observed near major cities such as Oslo, Bergen, and Kristiansand.

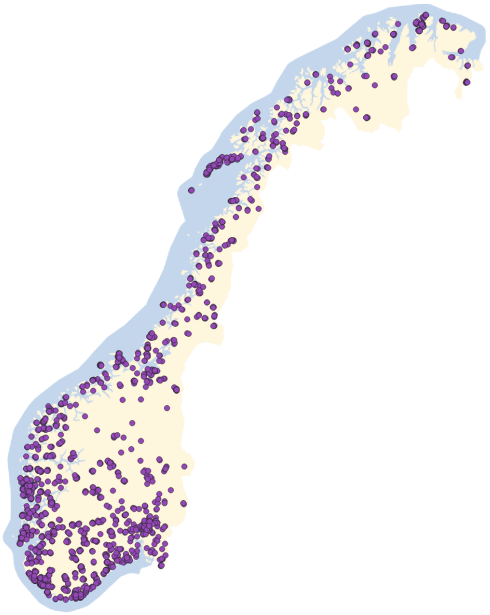

Figure 30: Center of lakes with grid connection located within a distance of 2 km. Source: Landscape and marine layers from Norwegian Mapping Authority [53]

Despite the stringent constrictions of scenario 4, the estimated energy yield of 2.6 TWh/year make up 28.3 % of the goal of 8 TWh/year solar energy by 2030. With the annual energy yield potential ranging from 247 kWh - 5.9 GWh, with the smallest system being 3 m^2 and the largest being 1.1 km^2. The average annual system yield was found to be 2.4 GWh.

Pairing floating solar photovoltaics with hydropower reservoirs has the potential to generate 20.4 TWh with a maximum of 25 % surface coverage while not exceeding the installed capacity of the hydro plant. None of the systems were limited by the capacity of the hydro plant.

4.1.1 Energy yield potential of market balancing area

Figure 31 presents a breakdown of the energy yield potential by market balancing area, providing insights into how the potential of FPV for scenario 4 and 5 is distributed across different market balancing areas.

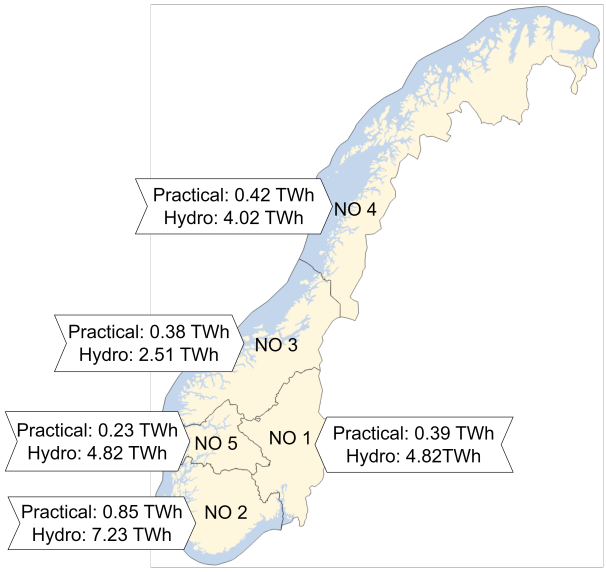

Figure 31: The annual energy yield potential concerning market balancing areas based on scenario 4 (practical) and 5 (hydro) . Source: Landscape and marine layers from Norwegian Mapping Authority [53], market balancing area layer from NVE [46].

Table 6: Comparison of market balancing areas: Consumption for 2023, and percentage of consumption that could potentially be covered by FPV based on scenario 4 (practical) and 5 (hydro). Consumption data origins from Elhub [3].

Market balancing area	Consumption 2023, [TWh]	Practical coverage, [%]	Hydro coverage, [%]
NO1	31 995	1.2	5.6
NO2	34 368	2.5	21.0
NO3	26 089	1.5	9.6
NO4	19 384	2.2	20.7
NO5	15 325	1.5	31.5
Total:	128 061	4.60	15.9

Table 6 complements this analysis by comparing the estimated energy yield to the electricity consumption in 2023 within each market balancing area. Notably, NO2 emerges as particularly promising, exhibiting the highest FPV potential of 2.2 TWh, a 6.40% coverage of the electricity consumption recorded for NO2 in 2023.

4.1.2 Energy yield potential of municipalities

Figure 32 maps the distribution energy yield potential of municipalities across Norway under scenarios 4 and 5, with the height of each bar representing the estimated gigawatt-hour (GWh) energy yield potential. In scenario 4, which imposes practical constraints on floating PV deployment, tends to show a more uniform distribution of energy yield potential across municipalities. In contrast, scenario 5, which focuses exclusively on floating PV deployment on hydroelectric reservoirs, municipalities exhibit a diverse range of energy potential, resulting in bars of varying heights. Municipalities with hydroelectric reservoirs generally exhibit higher energy yield potential compared to those without such infrastructure.

Table 7 presents the top 10 municipalities with the highest potential for installing floating PV systems based on the 4th scenario, which imposes practical constraints on FPV deployment. The municipalities are ranked according to their estimated FPV potential in gigawatt-hours (GWh) per year. Flekkefjord emerges as the municipality with the greatest potential, with an estimated FPV potential of 199.34 GWh/year. Other notable municipalities include Hábmer - Hamarøy, Kvinnherad, and Larvik. These findings provide valuable insights for decision-makers and stakeholders interested in prioritizing FPV installations in areas where practical considerations play a significant role.

Table 8 showcases the top 10 municipalities with the highest potential for installing floating PV systems on hydroelectric reservoirs, based on the 5th scenario. This scenario focuses exclusively on FPV deployment on hydro plant reservoirs, subject to capacity limitations and surface coverage restrictions. Suldal tops the list with an estimated FPV potential of 1336.67 GWh/year, followed by municipalities like Bykle, Vinje, and Ullensvang. These results highlight the significant energy generation potential of integrating FPV systems with existing hydro infrastructure, paving the way for sustainable energy solutions in these regions.

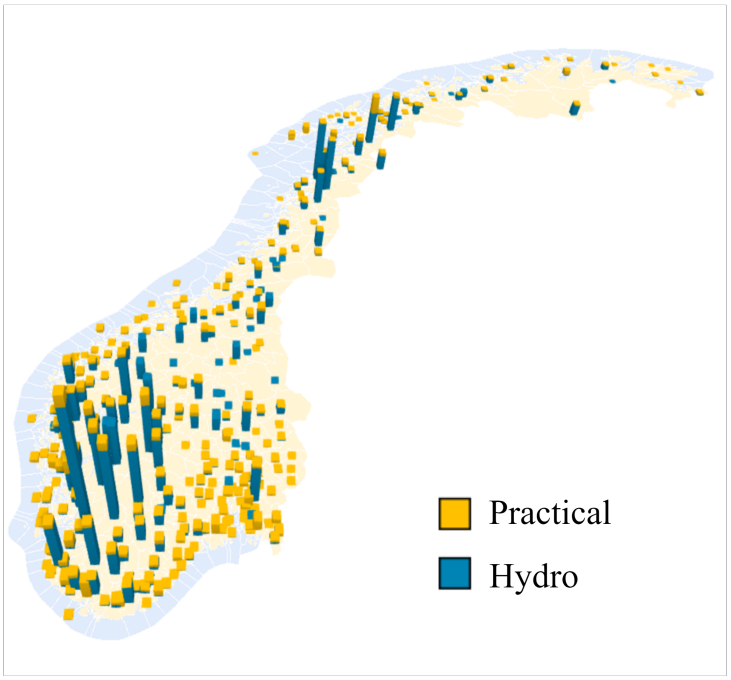

Figure 32: Map of estimated annual energy yield potential for scenario 4 (Pracical) and 5 (Hydro) concerning municipalities.

Table 7: Top 10 municipalities with the highest potential for installing floating PV systems in near future based on the 4^{th} scenario.

Municipality	FPV potential, [GWh/year]
Flekkefjord	199.34
Hábmer - Hamarøy	183.00
Kvinnherad	151.16
Larvik	132.51
Sarpsborg	121.38
Hol	114.09
Suldal	111.51
Nordre Follo	94.43
Strand	93.43
Vestvågøy	85.21

Table 8: Top 10 municipalities with the highest potential for installing floating PV systems on hydroelectric reservoirs based on the 5^{th} scenario.

Municipality	FPV potential, [GWh/year]
Suldal	1336.67
Bykle	841.99
Vinje	675.97
Ullensvang	637.08
Meløy	625.65
Hol	562.67
Rana	548.03
Luster	536.75
Sandnes	507.06
Sirdal	493.67

5 Discussion

The results obtained from the examination of lake areas and the estimation of energy yield potential shed light on several key aspects regarding the feasibility and implications of floating photovoltaic (FPV) deployment in Norway.

5.1 Maximizing energy potential while ensuring social acceptance

The study revealed a substantial energy production potential from FPV installations covering Norway's vast lake surfaces. However, to ensure social acceptance and environmental preservation, it became necessary to impose constraints on the extent of FPV deployment. This included limiting coverage to 10% of water bodies and excluding conserved or flood-prone areas. While these measures led to a significant reduction in available areas for FPV deployment, they align with principles of sustainable development and responsible resource management, with the capacity to generate 133 % of the Norwegian electricity consumption in 2023. This indicates that FPV installations hold promise as a viable renewable energy solution that can not only meet but exceed the nation's current energy demands.

However, solar energy production varies depending on factors like weather conditions and the time of year. This variability poses challenges for maintaining a consistent power supply during days and seasons.

As illustrated in Figure 13, solar production during the winter season is very low compared to the summer season. Effectively snow dissipation can smoothen out the variations between the summer and winter seasons. But for the production to be able to meet the demand, effective energy storage solutions are needed, especially for a grid system reliant on solar production as one of the primary energy sources, where solar energy can produce more than what is consumed. Technologies such as batteries, pumped hydro storage, and thermal energy storage can store excess energy generated during sunny periods for use when sunlight is scarce. Implementing these storage solutions alongside FPV installations can help mitigate the intermittency of solar power and ensure a reliable energy supply throughout the year.

Additionally, managing the voltage output from FPV installations can be challenging due to fluctuating sunlight intensity and changing weather conditions. To address this, advanced power electronics and control systems can be employed to regulate voltage levels and ensure grid stability.

5.2 Local Site Selection and Grid Connectivity

Installing powerplants far from consumption is both ineffective and increases the project's timeline. By prioritizing local FPV deployment sites, and having grid connectivity within a 2km distance, the systems are more probable. A total of 5250 lakes was identified to meet these criteria and were primarily clustered around coastal regions and major cities. These sites hold the potential to generate 30.9 TWh/year with a maximum of 10% surface coverage.

This strategic approach capitalizes on existing infrastructure and minimizes transmission losses, enhancing the efficiency and reliability of renewable energy integration into the grid. However, it might be a bit conservative approach, as there can be larger lakes worthy of investing a bit more on infrastructure to utilize larger available spots for deployment.

5.3 Potential for avoiding concession requirement

Focusing on achieving the goal of 8 TWh of solar production by 2030, avoiding the need for concession can expedite project timelines. Leveraging the Norwegian Water Resources and Energy Directorate's (NVE) recommendation of a 5 MW threshold for concession requirement can facilitate this. Our study indicates that systems falling below this threshold have the potential to generate 2.2 TWh annually, representing 28.3% of the revised budget plan for 2023 aimed at reaching the 8 TWh target by 2030.

This approach is significant as it not only accelerates project timelines but also enhances the likelihood of meeting the ambitious solar production goal within the stipulated timeframe. Moreover, opting for floating PV installations, which often bypass the need for concession, offers additional advantages. Floating PV systems are typically easier to implement and have

shorter installation timelines compared to land-based counterparts [4]. These factors further underscore the efficiency gains and expedited deployment achievable through the strategic utilization of floating solar technology.

5.4 Integration with hydropower reservoirs

Pairing FPV with hydropower reservoirs emerged as a promising strategy to optimize energy production and leverage existing infrastructure. With high energy prices and a decreasing solar cell price, it can be beneficial to invest in larger systems. This study indicates that deploying FPV exclusively on hydro plant reservoirs could generate 20.4 TWh/year with a maximum of 25% surface coverage while ensuring compliance with installed hydro capacity limits. This approach not only enhances renewable energy output but also promotes synergy between different clean energy sources, contributing to a more resilient and sustainable energy system.

5.5 Market balancing area

Figure 31 and Table 6 provide insights into the potential energy yield from Floating Photovoltaic (FPV) systems across Norway's market balancing areas. The data reveals the varying capacities of different regions to contribute to Norway's renewable energy goals based on their energy consumption and potential FPV output. For instance, NO1 has for the practical scenario a potential energy yield of 0.39 TWh/year, and for the scenario of FPV deployment on hydro reservoirs has a potential energy yield of 4.82 TWh/year. While NO2, which stands out as the most promising area, shows a practical yield of 0.85 TWh and a hydro yield of 7.23 TWh.

5.6 Limitations and drawbacks

When assessing the energy yield potential in Norway, this study encountered various challenges that influenced the overall performance of the assessment. This subsection explores the limitations associated with panel orientation, unwanted system placements, recreational activities, efficiency assessment, weather data accuracy, and grid capacity limitations.

5.6.1 Orientation of panels

The Python package used for finding the largest rectangles was axis-aligned, meaning that the sides aligned with the coordinate axis. As the simulated system was flat mounted, having 0° tilt, floating photovoltaic systems did not need to face south as simulated. A better approach could be using an arbitrary orientation as illustrated in Figure 33. Although comprehensive and computationally expensive, this application would find the absolute largest rectangle within the selected area.

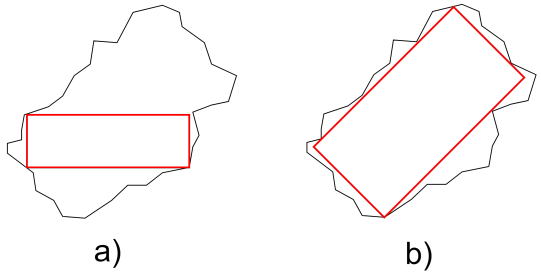

Figure 33: Finding the largest rectangle with (a) axis-aligned and (b) arbitrary orientation. Recreated from source: [63]

Finding the largest rectangle has its downsides. It risks covering an unrealistically large part of the coastline. The initial area might be unrealistic, but after constraining systems to have a maximum power output of 5 MW, the area is reduced to a more appropriate size.

Limiting the system areas to cover a max 10%, and reducing the size in ascending order on systems results if the largest systems get their area reduced due to the 5 MW constriction. An alternative method would have been to calculate energy yield before reducing the system areas.

Ensuring that no system occupies more than 10% of the lake area, system areas were reduced in ascending order. As this was done before the area reduction due to the 5 MW constriction, some lakes may end up covering less than 10%, when they have the possibility of having larger coverage. Another approach to solving this problem could involve assessing energy yield before adjusting system areas concerning lake coverage.

5.6.2 Coverage of islands and unwanted areas

The rectangular shapes used to represent FPV installations on lakes may unintentionally cover small

islands within the lake or lake area further than 300 m from the coastline. This can happen if the border of the installation intersects with these features, leading to suboptimal placement of FPV panels.

5.6.3 Lake usage for recreational activities

The practical area estimation for floating photovoltaic (FPV) systems may not fully account for the various activities that take place on lakes, such as fishing, swimming, and boating. These activities are often popular among local communities and tourists, and covering parts of the lake with FPV panels could potentially interfere with these recreational uses. In practice, when looking at the feasibility of FPV deployment, it is essential to consider the socio-economic and environmental impacts of FPV installations on recreational activities and to engage with the community to address their concerns. With the lack of incorporating this aspect into the analysis, it is expected that the locations found may not be ideal.

5.6.4 Actual efficiency of system

The accuracy of energy yield assessments for Floating Photovoltaic (FPV) systems depends on how well the model accounts for real-world variables. The current analysis uses a simplified model that may not fully capture the complexities of FPV performance.

In practice, derate factors, which account for efficiency losses, can fluctuate due to various environmental and operational factors. These include shading, wave activity, and temperature variations, all of which can significantly impact the system's power output. While the thermal model considers temperature fluctuations within the solar cells, it does not account for the effects on other system components. This oversight can lead to discrepancies between estimated and actual energy yields.

Soiling, or the accumulation of dirt on the panels, is another critical factor. The soiling parameters used in this analysis are derived from a limited number of locations and may not accurately reflect local variations. Consequently, the energy yield estimates might not fully capture the impact of soiling across different regions.

Additionally, variations in air mass throughout the day and across locations affect the ratio of high-energy to low-energy photons reaching the FPV panels. Higher proportions of high-energy photons can increase electron excitation but also cause more thermalization, leading to efficiency losses. The current model does not account for these variations, which can affect overall system performance.

The U-value, which measures the heat transfer rate, is another crucial parameter. The chosen U-value of $46\,\mathrm{W/m^2K}$ for this study assumes air-cooled panels and is based on experiments where solar panels were placed on plastic tubes over a floating membrane [14]. The U-value can vary significantly depending on the materials and design of the FPV system. Another study by IFE investigated U-values for a similar FPV system as illustrated in Figure 8, and found a median U-value of $33\,\mathrm{W/m^2K}$, with values ranging from $31\,\mathrm{W/m^2K}$ to $38\,\mathrm{W/m^2K}$ [64]. Given this variability, the U-value used in this study might be higher than an average of all FPV technologies. However, as these modules are only air cooled, without direct or indirect contact with the water surface, it can be reasonable that these panels have a lower U-value compared to FPV technologies like Ocean Sun or Sunlit Sea. Conducting an elasticity analysis to determine how changes in the U-value affect system performance would be beneficial. Adjusting the U-value based on empirical data and specific site conditions can enhance the accuracy of energy yield predictions.

Incorporating these factors into the analysis can significantly improve the reliability of energy yield assessments for FPV systems. By accounting for environmental variations, soiling rates, and precise U-values, it is possible to achieve more accurate and realistic energy predictions.

5.6.5 Significance of weather data

The accuracy of energy yield assessments for Floating Photovoltaic (FPV) systems is critically dependent on the quality of the weather data used in simulations. Accurate weather data ensures realistic predictions of solar irradiance, temperature, and other meteorological factors that directly influence the performance of solar panels.

This study was based on the weather models PVGIS-ERA5 and PVGIS-SARAH2, which have significant differences in spatial resolution and geographic cov-

erage. PVGIS-ERA5, with a resolution of approximately 31 km, provides extensive temporal coverage but may miss local weather variations essential for precise energy yield predictions, especially in areas with diverse topographies and microclimates. For instance, within a single 31 km grid cell, temperature and irradiance can vary significantly, affecting the energy output of FPV systems. In contrast, PVGIS-SARAH2 offers a finer resolution of 5.5 km, which captures local weather conditions more accurately but is limited to latitudes below 65° N, thus excluding the northernmost parts of Norway. However, since the spatial resolution of horizon data is much finer, at 90 m, variations in irradiance levels can occur within the grid cell, particularly during low solar altitudes. These variations influence the annual energy yield per unit area.

One crucial aspect not accounted for in the current models is the reflection of light from surrounding topography, which can significantly impact solar irradiance, particularly in mountainous regions during winter when snow cover is prevalent. This oversight can lead to underestimations of potential energy yields in these regions.

To enhance the accuracy of FPV energy yield estimations, it is essential to use higher-resolution weather models and incorporate ground-based observations. For example, the CARRA2 system (Copernicus Arctic Regional Reanalysis, second generation) offers a high resolution of 2.5 km and full coverage of Norway, providing a more detailed and accurate weather dataset. Comparing the estimated energy yields using different models, including CARRA2, can reveal significant differences and improve the reliability of the assessments.

Ultimately, the most precise approach would involve applying location-specific weather models based on directly measured values. This method would accurately reflect the unique weather conditions experienced at each site, thereby enhancing the reliability of energy yield predictions for FPV systems. By addressing these data quality issues, planners and developers can make more informed decisions, ensuring the effective deployment and operation of FPV systems in Norway.

5.6.6 Grid Capacity Limitations

This study has not taken into consideration that not all grid infrastructures may be capable of accommodating solar installations, such as 5 MW FPV systems. Grid capacity limitations, including transmission line constraints and voltage stability issues, may restrict the deployment of FPV projects in certain regions.

5.7 Limitation on maximum power output

Limiting the area so the maximum power output does not exceed 5 MW may not be the best approach. As reviewed in subsection 2.5.1, dynamic throttling can be used to limit the maximum power output of FPV systems during certain hours to avoid exceeding a predefined threshold, such as 5 MW. Having a dynamic control strategy could ensure grid stability and prevent overloading during peak production hours.

5.8 Possibility to exceed the socially acceptable area threshold

The socially accepted coverage percentage of 10% may not apply to all water bodies. While Norway may not be among the countries most prone to water scarcity, there have been occasions when unnecessary water consumption has been restricted. In light of global warming and that extreme weather events are expected to become more frequent, the occurrence of droughts is anticipated to become more common in the future [25]. To mitigate the impact, covering larger sections of drinking water reservoirs could effectively reduce water loss due to evaporation during these periods.

Given that certain drinking water sources in Norway suffer from high algae concentration and low water quality, covering a larger portion of the water body may contribute to quality improvement, subsequently diminishing the need for chemicals to detoxify the water.

5.9 Applications for development in preserved areas

Even if the areas are protected, it is possible to apply for exceptions from the conservation regulations. An

analysis by Natur & miljø (Nature & Environment) reveals that 94 percent of applicants are granted permission for a range of activities, including constructing buildings, driving, extracting materials, engaging in fish farming, mining, and other practices within Norwegian conservation areas [65].

5.10 Tilt vs no tilt

The use of no tilt can have both advantages and drawbacks.

A study done on pairing floating solar photovoltaics with hydropower reservoirs in Europe stated that when the system size is limited by a maximum power, having flat panels and not tilted panels would give the same power output [29].

Having tilted panels would reduce the angle of irradiance, thereby minimizing reflection losses and maximizing the efficiency of solar energy capture. Comparing a larger flat FPV system to a smaller tilted one, the

However, this advantage must be balanced against the potential drawbacks associated with tilted panels.

Tilted panels can cause shading effects, particularly during periods of low solar altitudes. For higher solar altitudes, there is a risk of some solar irradiance being lost between the panels, thereby diminishing overall energy production potential.

Moreover, while tilted panels may benefit from increased convective cooling due to their elevated position, this advantage is contingent upon wind direction. Introducing tilt can result in a turbulent wind profile, potentially disrupting the uniformity of convective cooling across the solar array. Panels situated in the first row may act as a windshield for those positioned behind them, leading to uneven distribution of convective cooling. This uneven cooling profile can exacerbate mismatch losses within the system, ultimately impacting overall energy yield and efficiency.

Furthermore, it's essential to consider the impact of snow coverage on tilted panels. Snow accumulation on tilted panels can slide off more easily compared to flat panels, mitigating the risk of reduced energy production due to snow coverage. Additionally, the design of bifacial panels, which can produce energy from both the front and rear sides, presents an intriguing advantage. In snowy conditions, the rear side of bifacial panels can generate heat during energy production as it is not covered by snow. As a result, the internal thermalization process within the panels generates heat, which aids in melting snow accumulation on the front side.

5.11 Hydro power

The water reservoirs associated with hydroelectric plants have already been affected by human intervention, making them suitable for additional exploitation. Instead of constraining the max power concerning the grid capacity, the threshold could be set dependent on the hydroelectric capacity, as the hydroelectric power plant could be used to adjust the net power delivered to the grid. Despite potential challenges such as increased mooring costs due to dynamic water levels, the expansive surface area offered by reservoirs together with the possibility of balancing production can facilitate the deployment of large-scale floating PV plants. This balance enables cost reduction in overall power generation.

The system operator of the Norwegian power system, Statnett, is expecting a power shortage from 2027 [66]. At the same time Norway is expecting a record number of negative electricity prices [67]. As the country transitions towards a more renewable energy-focused grid, the intermittency of renewable sources like wind and solar power emphasizes the urgency of implementing effective storage technologies. A market where the producers have to pay to get rid of the generated energy, is not very desirable. In times of negative or low prices hydroelectric plants can pump water into their reservoir, which can be released later when demand is high or prices are favorable.

Furthermore, the ability of hydroelectric plants to shift between generation and pumping modes allows them to adapt to market conditions dynamically. By strategically pumping water during periods of negative prices and selling electricity during peak demand hours, hydroelectric operators can optimize revenue generation while contributing to grid stability.

This dual role of hydroelectric plants not only provides a solution to the challenges posed by intermittent renewable energy sources but also offers economic benefits to power producers.

6 Conclusion

Floating photovoltaic (FPV) systems offer a significant opportunity for Norway to enhance its renewable energy portfolio and meet its ambitious target of generating 8 TWh of solar energy by 2030. This study demonstrates that FPV installations, especially when strategically integrated with existing hydropower infrastructure, can contribute substantially to this goal.

Theoretical modeling indicates that if 100% of Norway's lake surfaces were covered with FPV systems, the maximum potential energy yield could reach up to 1970 TWh annually. However, practical considerations, such as environmental constraints and social acceptance, adjust this potential to a more feasible 171 TWh/year when limiting coverage to 10% of lake surfaces and avoiding nature-reserved and flood-prone areas.

Focusing on FPV systems within 2 km of substations further refines this potential to approximately 30.9 TWh/year, emphasizing the importance of grid proximity for cost-effective energy generation. Smaller-scale installations under 5 MW, which do not require concessions, show a potential yield of up to 2.2 TWh/year, covering a significant portion of the national solar energy target and facilitating faster deployment.

Integrating FPV systems with hydropower reservoirs is particularly advantageous, offering a potential yield of 20.4 TWh/year at 25% coverage. This integration not only leverages existing infrastructure but also balances the variable output of solar power with the regulated flow of hydropower, enhancing overall grid stability and efficiency.

However, several challenges need to be addressed to fully realize the potential of FPV systems. These include ensuring reliable grid connectivity, mitigating environmental impacts, and managing higher operational costs compared to land-based PV systems. Technological advancements in power electronics and energy storage solutions, such as batteries and pumped hydro storage, are essential to address these challenges.

In conclusion, FPV systems hold great promise for contributing to Norway's renewable energy goals. By addressing the identified challenges and leveraging strategic advantages, FPV technology can play a critical role in creating a sustainable and resilient energy future for Norway.

7 Further Work

1. **Optimization of FPV Design for Nordic Conditions:**
    - Investigate the impact of extreme weather conditions (e.g., snow, ice, and wind) on FPV system performance and durability.
    - Develop and test new FPV designs that can withstand harsh Nordic climates and ensure year-round operation.
2. **Environmental Impact Assessment:**
    - Conduct comprehensive studies on the long-term environmental impacts of FPV installations on aquatic ecosystems.
    - Explore mitigation strategies for potential negative effects on water quality, aquatic life, and local biodiversity.
3. **Economic Feasibility and Incentives:**
    - Analyze the cost-benefit ratio of FPV systems compared to other renewable energy sources.
    - Develop economic models to assess the financial viability of FPV projects, including potential subsidies, tax incentives, and funding opportunities.
4. **Technological Advancements:**
    - Investigate advancements for various construction methods to improve the efficiency and longevity of FPV systems.
    - Explore the use of bifacial panels, advanced mooring systems, and tracking mechanisms to enhance energy yield.
5. **Grid Integration and Stability:**
    - Study the impact of large-scale FPV deployment on grid stability and develop solutions for managing variable solar output.
    - Research advanced power electronics, smart inverters, and energy storage solutions to optimize grid integration.
6. **Energy Storage Solutions:**
    - Evaluate the effectiveness of different energy storage systems, such as batteries and pumped hydro storage, in conjunction with FPV systems.
    - Investigate strategies for using excess solar energy to pump water back into hydropower reservoirs during periods of low demand.
7. **Societal Acceptance and Stakeholder Engagement:**
    - Conduct surveys and stakeholder workshops to understand public perception and acceptance of FPV systems.
    - Develop community engagement strategies to address concerns and highlight the benefits of FPV installations.
8. **Pilot Projects and Case Studies:**
    - Implement pilot FPV projects in various Norwegian regions to gather real-world performance data and refine deployment strategies.
    - Document case studies to share best practices and lessons learned from early adopters of FPV technology.
9. **Comprehensive Data Collection and Validation:**
    - Enhance weather models including water surface temperature for more accurate modeling and prediction of FPV performance.
    - Validate simulation models with real-world data from existing FPV installations to improve accuracy and reliability.

References

[1] "Revidert nasjonalbudsjett 2023 - enighet sv og regjering," Sosialistisk Venstreparti. (2023), [Online]. Available: https://www.sv.no/wp-content/uploads/2023/06/rnb-2023-enighet-apspsv-verbaler-rettet-1310.pdf (visited on 04/11/2024).

[2] NVE. "Nve anbefaler at solkraftanlegg opp til 5 mw ikke trenger konsesjon." (2024), [Online]. Available: https://www.nve.no/nytt-fra-nve/nyheter-energi/nve-anbefaler-at-solkraftanlegg-opp-til-5-mw-ikke-trenger-konsesjon/ (visited on 03/11/2024).

[3] Elhub. "Forbruk, produksjon og installert effekt." (2024), [Online]. Available: https://elhub.no/data/forbruk-og-produksjon/ (visited on 04/01/2024).

[4] World Bank Group, ESMAP and SERIS, *Where sun meets water: floating solar handbook for practitioners*. Washington, DC: World Bank, 2019, Accessed 12-27-2023.

[5] World Bank Group, ESMAP and SERIS, *Where sun meets water: floating solar market report*. Washington, DC: World bank, 2019, Accessed 12-18-2023.

[6] "Vast norwegian expertise perfect for floating solar," Business Norway. (), [Online]. Available: https://businessnorway.com/articles/enormous-potential-in-floating-solar (visited on 05/03/2024).

[7] "Enormt potensiale i flytende sol," Innovasjon Norge. (2023), [Online]. Available: https://www.innovasjonnorge.no/artikkel/enormt-potensiale-i-flytende-sol (visited on 05/03/2024).

[8] "Projects," Ocean Sun. (), [Online]. Available: https://oceansun.no/projects/ (visited on 04/10/2024).

[9] S. Sea. "Technology." (), [Online]. Available: https://sunlitsea.no/technology (visited on 03/27/2024).

[10] D. J. MacKay, *Sustainable Energy-without the hot air*. Elsevier Ltd, 2009, ISBN: 978-0-9544529-3-3.

[11] A. Smets, K. Jãger, O. Isabella, R. V. Swaaij, and M. Zeman, *Solar energy*. UIT Cambridge Ltd, 2016, ISBN: 978 1 906860 32 5.

[12] M. A. Brandsrud, R. Blümel, C. C. You, *et al.*, "An exact ray model for oblique incident light on planar films," *Physica E: Low-Dimensional Systems and Nanostructures*, vol. 126, Feb. 2021, ISSN: 13869477. DOI: 10.1016/j.physe.2020.114374.

[13] H. Heidarzadeh, A. Rostami, and M. Dolatyari, "Management of losses (thermalization-transmission) in the si-qds inside 3c–sic to design an ultra-high-efficiency solar cell," *Materials Science in Semiconductor Processing*, vol. 109, p. 104 936, 2020, ISSN: 1369-8001. DOI: https://doi.org/10.1016/j.mssp.2020.104936. [Online]. Available: https://www.sciencedirect.com/science/article/pii/S1369800119311606.

[14] T. Kjeldstad, D. Lindholm, E. Marstein, and J. Selj, "Cooling of floating photovoltaics and the importance of water temperature," *Solar Energy*, vol. 218, pp. 544–551, Apr. 2021, ISSN: 0038092X. DOI: 10.1016/j.solener.2021.03.022.

[15] W. Z. Leow, Y. M. Irwan, M. Asri, *et al.*, "Investigation of solar panel performance based on different wind velocity using ansys," *Indonesian Journal of Electrical Engineering and Computer Science*, vol. 1, pp. 456–463, 3 Mar. 2016, ISSN: 25024760. DOI: 10.11591/ijeecs.v1.i3.pp456-463.

[16] M. Dörenkämper, A. Wahed, A. Kumar, M. de Jong, J. Kroon, and T. Reindl, "The cooling effect of floating pv in two different climate zones: A comparison of field test data from the netherlands and singapore," *Solar Energy*, vol. 214, pp. 239–247, Jan. 2021, ISSN: 0038092X. DOI: 10.1016/j.solener.2020.11.029.

[17] "How does floating solar power system work?" SunEvo Solar. (2022), [Online]. Available: https://www.sunevosolar.com/blog/how-does-floating-solar-power-system-work_b9 (visited on 04/10/2024).

[18] "Technology in floating pv develops a key role in long term approach for sustainability within the renewables energy sectors," SunEvo Solar. (2023), [Online]. Available: https://www.solarisfloat.com/technology-in-floating-pv-develops-a-key-role-in-long-term-approach-for-sustainability-within-the-renewables-energy-sectors/ (visited on 04/10/2024).

[19] S. Natarajan, A. Kumar, R. Mohamed, R. Rathna, S. Mondal, and S. K. Suraparaju, "Design and development of dual axis sun tracking system for floating pv plant," *IOP Conference Series: Earth and Environmental Science*, vol. 312, p. 012 001, Oct. 2019. DOI: 10.1088/1755-1315/312/1/012001.

[20] E. Skoplaki and J. A. Palyvos, "Operating temperature of photovoltaic modules: A survey of pertinent correlations," *Renewable Energy*, vol. 34, pp. 23–29, 1 Jan. 2009, ISSN: 09601481. DOI: 10.1016/j.renene.2008.04.009.

[21] A. Rajmani and P. Guha, "Analysis of wind & earthquake load for different shapes of high rise building," 2015. [Online]. Available: https://api.semanticscholar.org/CorpusID:111175079.

[22] F. Bañuelos-Ruedas, C. Angeles-Camacho, and S. Rios-Marcuello, *Analysis and validation of the methodology used in the extrapolation of wind speed data at different heights*, 2010. DOI: 10.1016/j.rser.2010.05.001.

[23] N. Gjølme, T. Krogh, and H. Utkilen, *Cyanobakterier (blågrønnalger) oppblomstring og toksinproduksjon rapport 2010:4*. 2010, ISBN: 9788280824349. [Online]. Available: www.fhi.no.

[24] R. Sirevåg. "Blågrønnbakterier," Store Norske Leksikon. (2023), [Online]. Available: https://snl.no/bl%C3%A5gr%C3%B8nnbakterier (visited on 05/03/2024).

[25] J. L. vei, A. Hindar, Ø. Garmo, K. Austnes, and J. E. S. F. S. nedbør Distribusjon, *Nasjonal innsjøundersøkelse 2019*, ISBN: 9788257772659. [Online]. Available: www.niva.no.

[26] B. Figgis, G. Scabbia, and B. Aissa, "Condensation as a predictor of pv soiling," *Solar Energy*, vol. 238, pp. 30–38, 2022, ISSN: 0038-092X. DOI: https://doi.org/10.1016/j.solener.2022.04.025. [Online]. Available: https://www.sciencedirect.com/science/article/pii/S0038092X22002730.

[27] D. Khademaljamea, I. Masalha, A. S. Alsabagh, O. Badran, and H. Maaitah, "Investigation on water immersing and spraying for cooling pv panel," *International Review of Mechanical Engineering (IREME)*, vol. 16, Jan. 2023. DOI: 10.15866/ireme.v16i9.22680.

[28] TUM. "Solceller er en kjempeutfordring for nettselskapene – slik skal problemet løses." (), [Online]. Available: https://www.tu.no/tumstudio/solceller/annonse-solceller-er-en-kjempeutfordring-for-nettselskapene-slik-skal-problemet-loses/521501 (visited on 04/09/2024).

[29] G. Kakoulaki, R. G. Sanchez, A. G. Amillo, *et al.*, "Benefits of pairing floating solar photovoltaics with hydropower reservoirs in europe," *Renewable and Sustainable Energy Reviews*, vol. 171, Jan. 2023, ISSN: 18790690. DOI: 10.1016/j.rser.2022.112989.

[30] L. Micheli, Á. F. Solas, E. F. Fernández, and N. Riedel-Lyngskaer, "The impact of soiling in europe: Estimation and error induced by typical loss assumptions," 2023. DOI: 10.4229/EUPVSEC2023/4AO.9.3. [Online]. Available: https://www.researchgate.net/publication/375967358.

[31] M. Øgaard and H. N. Riise. "Clean tuesday: Solenergi i norske forhold; soiling- og snøtap i norge," IFE. (2024), [Online]. Available: https://solenergiklyngen.no/event/clean-tuesday-solenergi-i-norske-forhold/ (visited on 02/13/2024).

[32] DNV GL, *Recommended practice: design, development and operation of floating solar photovoltaic systems*. DNV GL, 2021, Accessed 12-27-2023.

[33] A. Ghosh, *A comprehensive review of water based PV: Flotavoltaics, under water, offshore & canal top*. Elsevier Ltd., 2023, Accessed 10-01-2024.

[34] Z. Liu, C. Ma, X. Li, Z. Deng, and Z. Tian, "Aquatic environment impacts of floating photovoltaic and implications for climate change challenges," *Journal of Environmental Management*, vol. 346, Nov. 2023, ISSN: 10958630. DOI: 10.1016/j.jenvman.2023.118851.

[35] P.-A. Château, R. F. Wunderlich, T.-W. Wang, H.-T. Lai, C.-C. Chen, and F.-J. Chang, "Mathematical modeling suggests high potential for the deployment of floating photovoltaic on fish ponds," 2019. DOI: 10.1016/j.scitotenv.2019.05.420.

[36] I. Grigoriadou, K. Paraskevopoulos, K. Chrissafis, E. Pavlidou, T.-G. Stamkopoulos, and D. N. Bikiaris, "Effect of different nanoparticles on hdpe uv stability," *Polymer Degradation and Stability*, vol. 96, pp. 151–163, 1 Jan. 2011, ISSN: 01413910. DOI: 10.1016/j.polymdegradstab.2010.10.001.

[37] Miljødirektoratet. "Norges verneområder." (), [Online]. Available: https://www.miljodirektoratet.no/ansvarsomrader/vernet-natur/norges-verneomrader/ (visited on 02/22/2024).

[38] M. Bakkan, P. L. B. (Rambøll/NVE), T. E. Bønsnes, *et al.*, *NVE Veileder 3/2022: Sikkerhet mot flom. Utredning av flomfare i reguleringsplan og byggesak*, ISBN: 9788241022791. [Online]. Available: https://publikasjoner.nve.no/veileder/2022/veileder2022_03.pdf.

[39] B. Ellingsen. "Neste flomkrise: Ekspertene forbereder seg ved hjelp av satellitter," forskning.no. (2023), [Online]. Available: https://www.forskning.no/flom-informasjonsteknologi-norsk-romsenter/neste-flomkrise-ekspertene-forbereder-seg-ved-hjelp-av-satellitter/2239531 (visited on 04/09/2024).

[40] N. Naturskadepool. "Rundt 10 000 innmeldte skader etter ekstremværet «hans»." (2023), [Online]. Available: https://www.naturskade.no/nyheter/2023/rundt-10-000-innmeldte-skader-etter-ekstremvaret-hans/ (visited on 04/09/2024).

[41] "Produktark: Flom aktsomhetsområder," NVE. (2020), [Online]. Available: https://gis3.nve.no/metadata/produktark/Produktark_aktsomhetsomrader_flom_01092020.pdf.

[42] E. Skoplaki and J. A. Palyvos, "On the temperature dependence of photovoltaic module electrical performance: A review of efficiency/power correlations," *Solar Energy*, vol. 83, pp. 614–624, 5 May 2009, ISSN: 0038092X. DOI: 10.1016/j.solener.2008.10.008.

[43] D. Faiman, "Assessing the outdoor operating temperature of photovoltaic modules," *Progress in Photovoltaics: Research and Applications*, vol. 16, pp. 307–315, 4 Jun. 2008, ISSN: 10627995. DOI: 10.1002/pip.813.

[44] N. Riedel-Lyngskær, A. A. S. Lancia, F. Plag, *et al.*, "Interlaboratory comparison of angular-dependent photovoltaic device measurements: Results and impact on energy rating," *Progress in Photovoltaics: Research and Applications*, vol. 29, pp. 315–333, 3 Mar. 2021, ISSN: 1099159X. DOI: 10.1002/pip.3365.

[45] Sandia. "Ashrae iam model." (), [Online]. Available: https://pvpmc.sandia.gov/modeling-guide/1-weather-design-inputs/shading-soiling-and-reflection-losses/incident-angle-reflection-losses/ashrae-iam-model/ (visited on 03/12/2024).

[46] NVE. "Nedlasting av fagdata fra nve." (), [Online]. Available: https://nedlasting.nve.no/gis/ (visited on 01/11/2024).

[47] NVE. "Vassdragsdata." (2021), [Online]. Available: https://www.nve.no/kart/kartdata/vassdragsdata/ (visited on 04/01/2024).

[48] Geonorge. "N50 kartdata." (2024), [Online]. Available: https://register.geonorge.no/det-offentlige-kartgrunnlaget/n50-kartdata/ea192681-d039-42ec-b1bc-f3ce04c189ac (visited on 04/01/2024).

[49] "Sosi produktspesifikasjon produktnavn: N50 kartdata-versjon 20230401 produktspesifikasjon for n50 kartdata." version 20230401, Norwegian Mapping Authority (Kartverket). (2023), [Online]. Available: https://dokument.geonorge.no/produktspesifikasjoner/n50-kartdata/Versjon%20april%202023/produktspesifikasjon-n50-kartdata-versjon-april-2023.pdf.

[50] "Produktark: Nettanlegg," NVE. (2019), [Online]. Available: https://gis3.nve.no/metadata/produktark/produktark_nettanlegg.pdf.

[51] Kartverket. "Det offentlige kartgrunnlaget." (2023), [Online]. Available: https://www.kartverket.no/geodataarbeid/dok-og-temadata/det-offentlige-kartgrunnlaget (visited on 04/01/2024).

[52] NVE. "Nve kraftsystem nettanlegg." (), [Online]. Available: https://temakart.nve.no/tema/nettanlegg (visited on 04/05/2024).

[53] "Norges maritime grenser, illustrasjonskart," 2023. [Online]. Available: https://kartkatalog.geonorge.no/metadata/norges-maritime-grenser-illustrasjonskart/870d142b-a8fd-4f26-9c72-948d79c1a454 (visited on 04/03/2024).

[54] "Produktark: Naturvernområder," The Norwegian Environment Agency (Miljødirektoratet). (2020), [Online]. Available: https://register.geonorge.no/data/documents/Produktark_naturvernomrade_v1_naturvernomrader_.pdf.

[55] "Produktark: Vannkraft, utbygd og ikke utbygd," NVE. (2018), [Online]. Available: https://gis3.nve.no/metadata/produktark/produktark_vannkraft.pdf.

[56] Statnett. "Derfor har vi prisområder for strøm i norge." (2022), [Online]. Available: https://www.statnett.no/om-statnett/bli-bedre-kjent-med-statnett/om-strompriser/fakta-om-prisomrader/ (visited on 04/05/2024).

[57] Geonorge. "Administrative enheter kommuner." (2024), [Online]. Available: https://kartkatalog.geonorge.no/metadata/administrative-enheter-kommuner/041f1e6e-bdbc-4091-b48f-8a5990f3cc5b.

[58] E. Commission. "Pvgis user manual." (), [Online]. Available: https://joint-research-centre.ec.europa.eu/photovoltaic-geographical-information-system-pvgis/getting-started-pvgis/pvgis-user-manual_en (visited on 03/19/2024).

[59] o. o. C. European Centre for Medium-Range Weather Forecasts, "Era5: Data documentation," 2024. DOI: 10.21957/vhe0zlxr8.

[60] H. N. Riise, A. Dobler, B. Aarseth, M. M. Nygård, and E. Berge. "Clean tuesday: Solenergi i norske forhold; pvgis eller meteonorm?" IFE. (2024), [Online]. Available: https://solenergiklyngen.no/event/clean-tuesday-solenergi-i-norske-forhold/ (visited on 02/13/2024).

[61] J. Trentmann, U. Pfeifroth, S. Kothe, R. Hollmann, and M. Werscheck, "Product user manual meteosat climate data records of surface radiation sarah-2," 2017. DOI: 10.5676/EUM_SAF_CM/SARAH/V002.

[62] B. Marion, J. Adelstein, K. Boyle, *et al.*, *Performance parameters for grid-connected pv systems*, 2005. [Online]. Available: www.task2.org..

[63] R. Molano, P. G. Rodríguez, A. Caro, and M. L. Durán, "Finding the largest area rectangle of arbitrary orientation in a closed contour," *Applied Mathematics and Computation*, vol. 218, pp. 9866–9874, 19 Jun. 2012, ISSN: 00963003. DOI: 10.1016/j.amc.2012.03.063.

[64] T. Kjeldstad, V. S. Nysted, M. Kumar, *et al.*, "The performance and amphibious operation potential of a new floating photovoltaic technology," *Solar Energy*, vol. 239, pp. 242–251, Jun. 2022, ISSN: 0038092X. DOI: 10.1016/j.solener.2022.04.065.

[65] T. B. Christensen. "9 av 10 får bygge i vernet natur." (2023), [Online]. Available: https://naturvernforbundet.no/9-av-10-far-bygge-i-vernet-natur/ (visited on 02/23/2024).

[66] "Økende forbruk gir kraftunderskudd fra 2027," 2024. [Online]. Available: https://www.statnett.no/om-statnett/nyheter-og-pressemeldinger/nyhetsarkiv-2022/kortsiktig-markedsanalyse-okende-forbruk-gir-kraftunderskudd-fra-2027/ (visited on 05/14/2024).

[67] "Dette året gir antakelig rekordmange negative priser. hva betyr det for produsentene?" europower. (2024), [Online]. Available: https://www.europower.no/kraftmarked/dette-aret-gir-antakelig-rekordmange-negative-priser-hva-betyr-det-for-produsentene-/2-1-1643019 (visited on 05/14/2024).

[68] Kartverket. "Kvar er midtpunktet i noreg?" (2024), [Online]. Available: https://kartverket.no/til-lands/fakta-om-norge/noregs-midtpunkt.

A Geospatial data

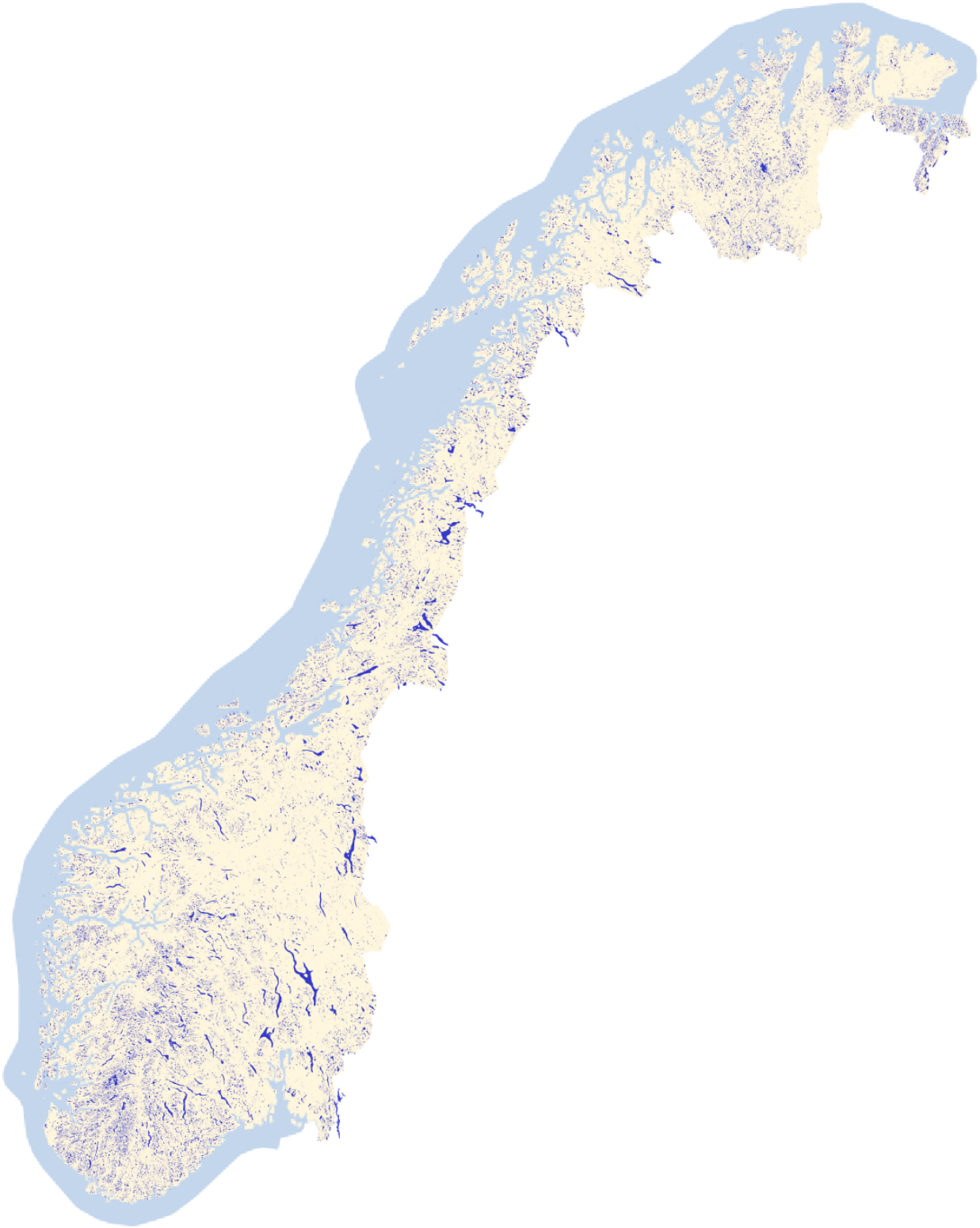

Figure 34: Map of all lakes in Norway. Source: NVE (data) [46], The Norwegian Mapping Authority (background) [53].

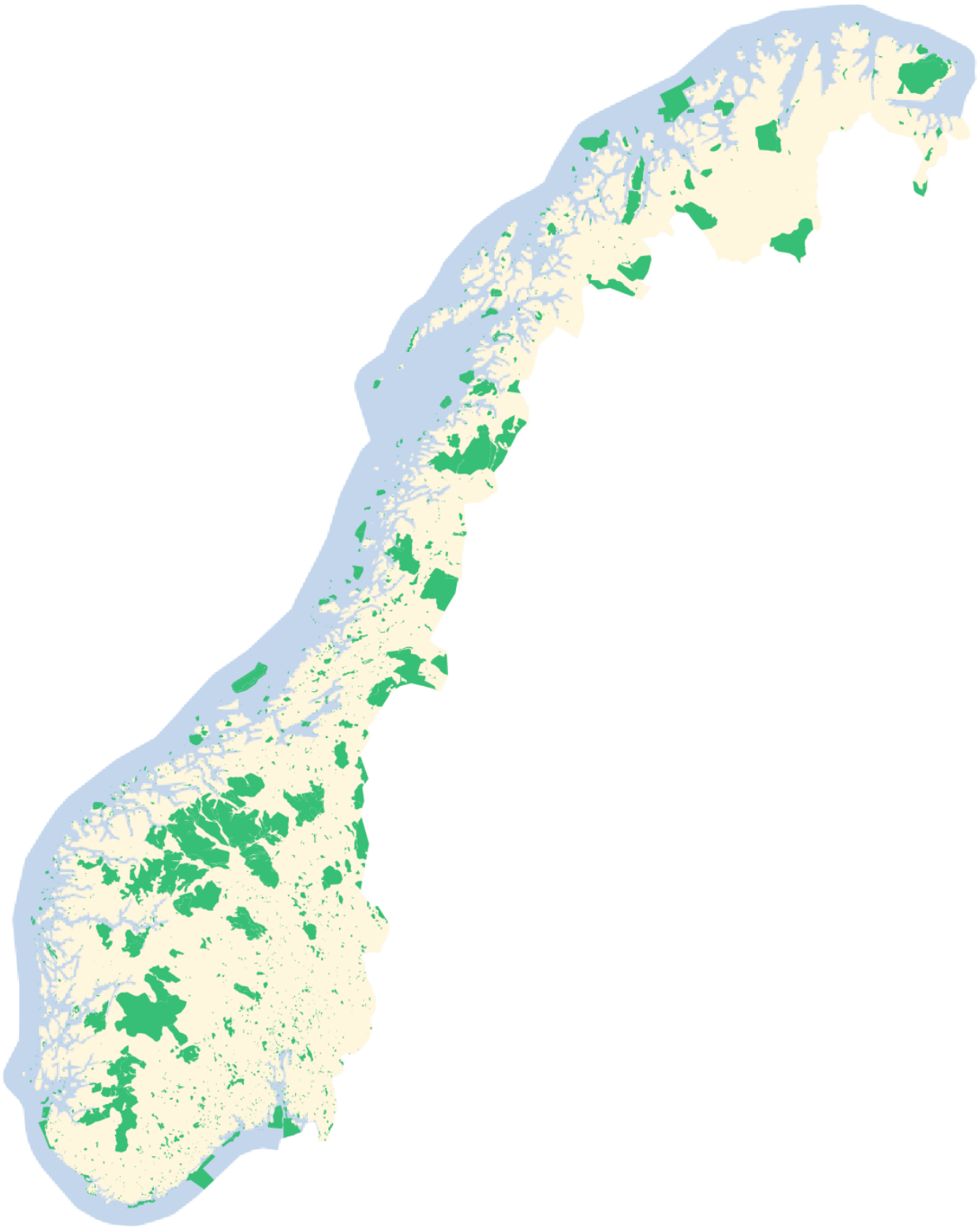

Figure 35: Mapping of conserved areas in Norway. Source: NVE (data) [46], The Norwegian Mapping Authority (background) [53].

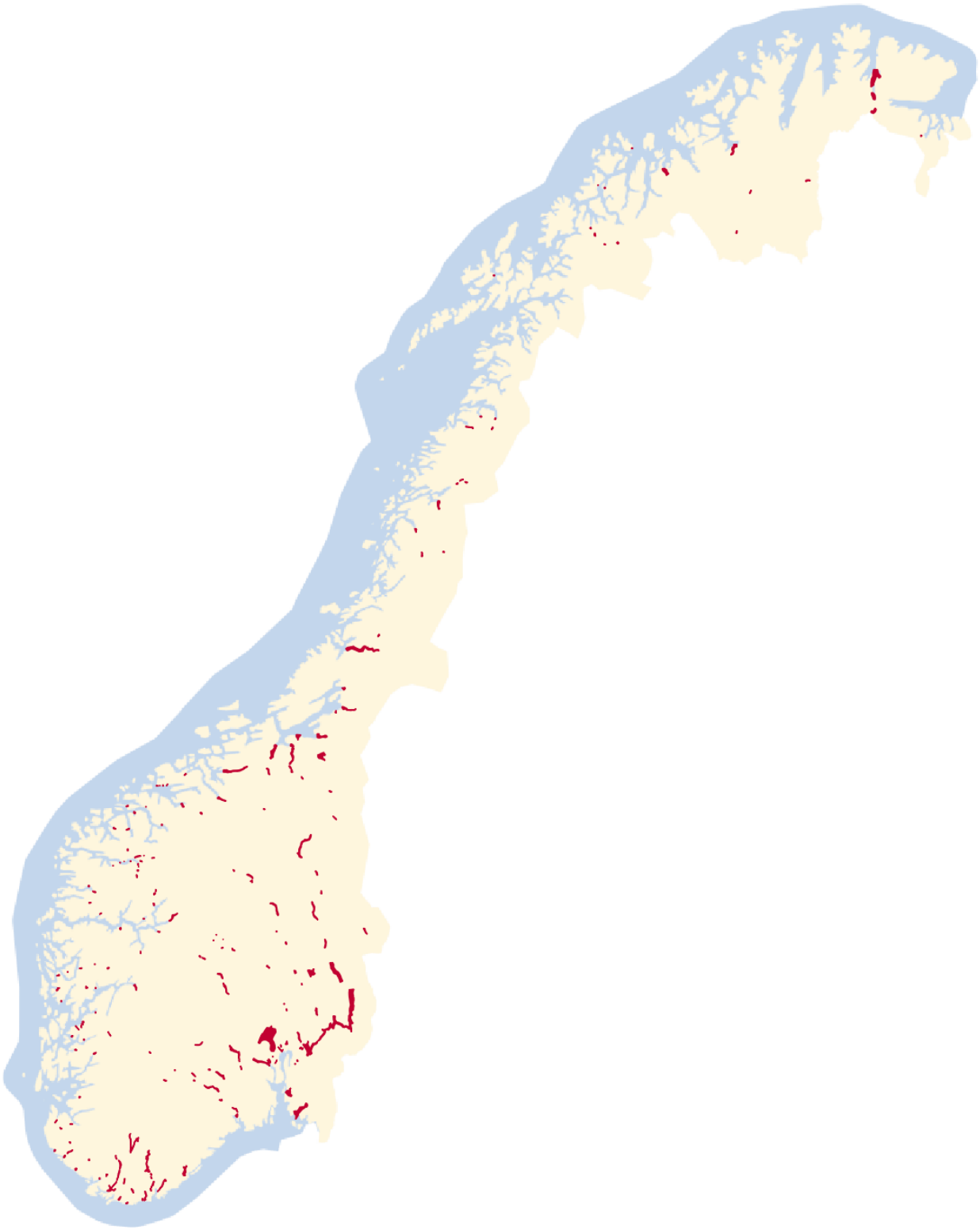

Figure 36: Flood hazard areas in Norway.Source: NVE (data) [46], The Norwegian Mapping Authority (background) [53].

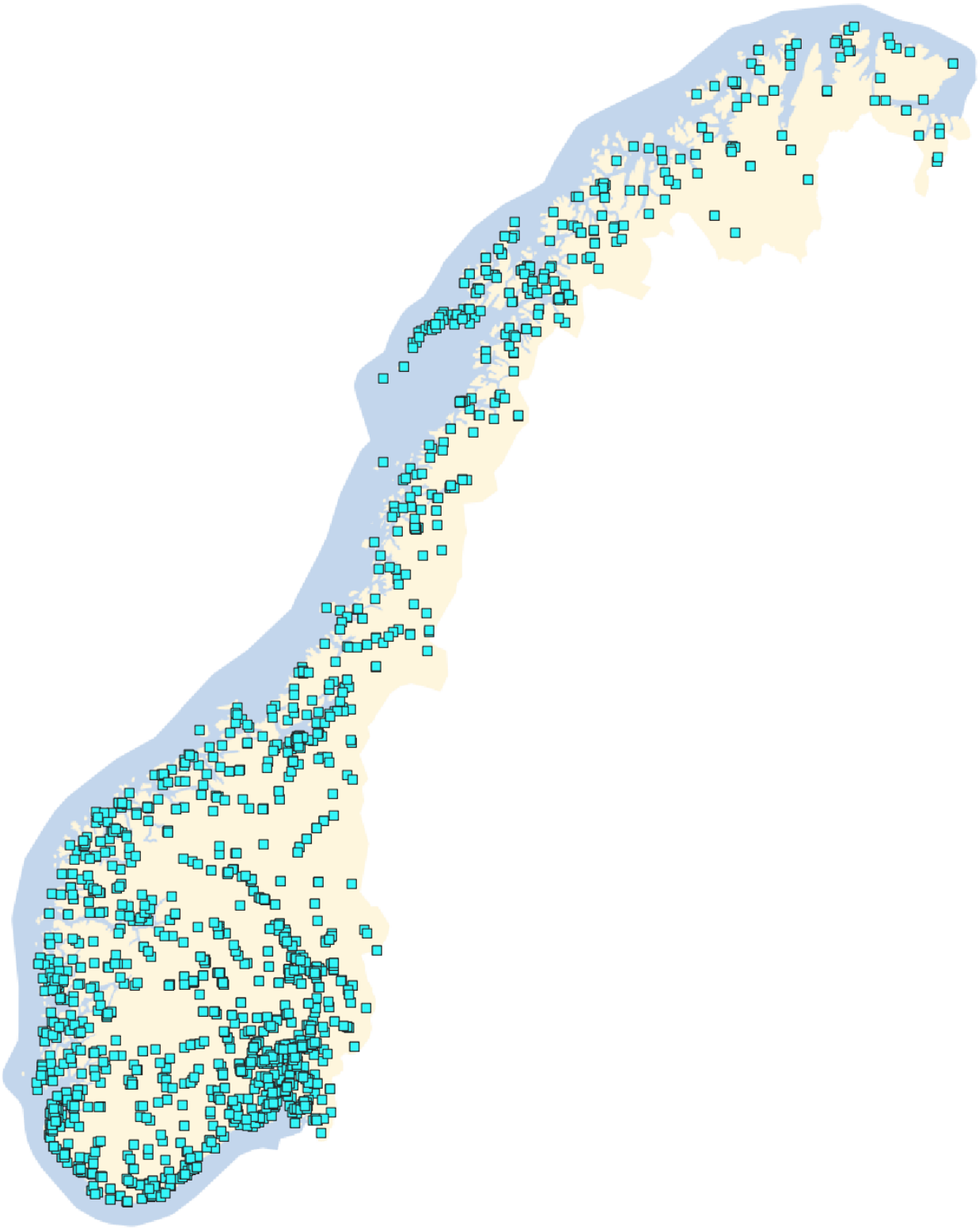

Figure 37: Map of Norwegian substations.Source: NVE (data) [46], The Norwegian Mapping Authority (background) [53].

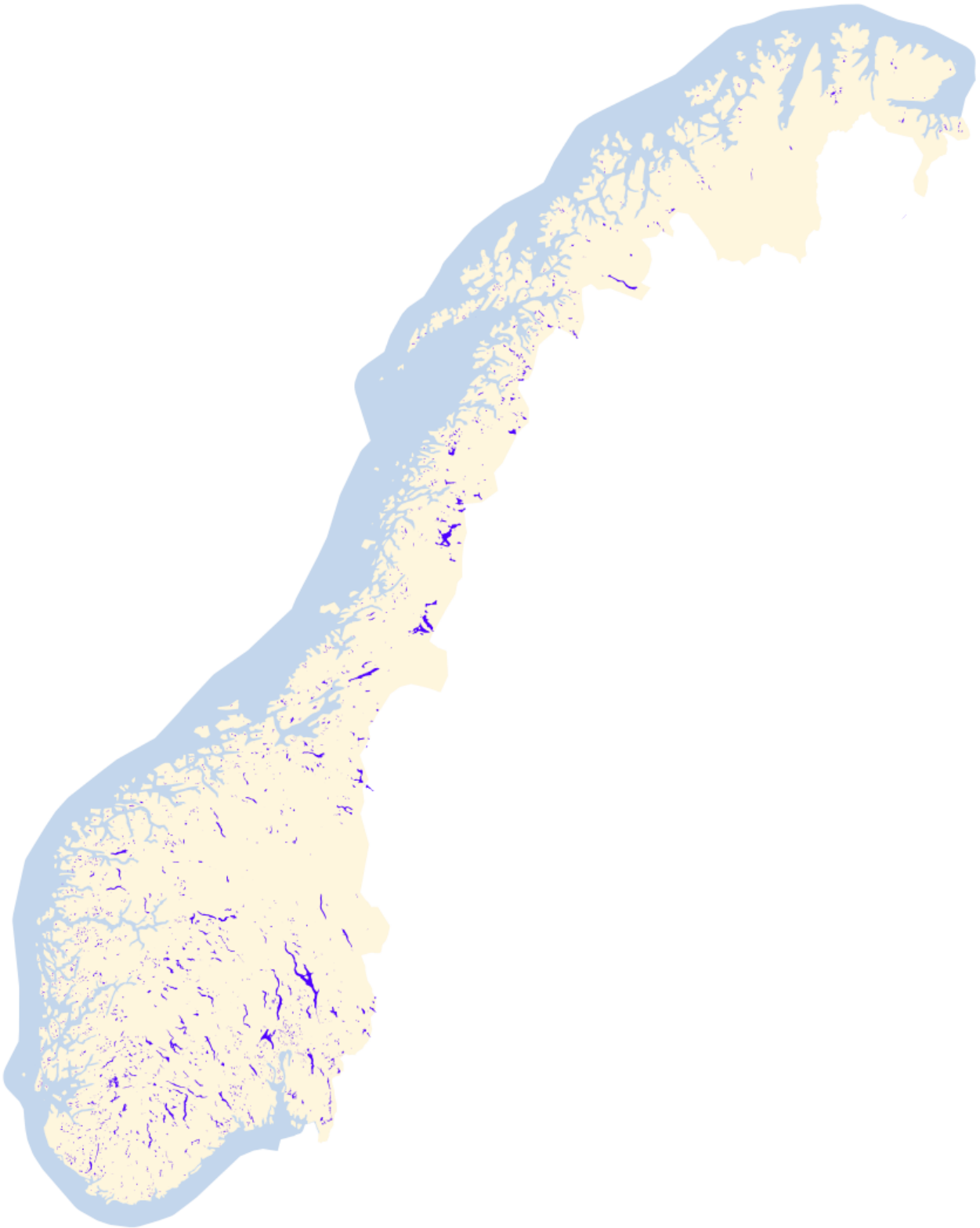

Figure 38: Map of regulated reservoirs in Norway. Source: NVE (data) [46], The Norwegian Mapping Authority (background) [53].

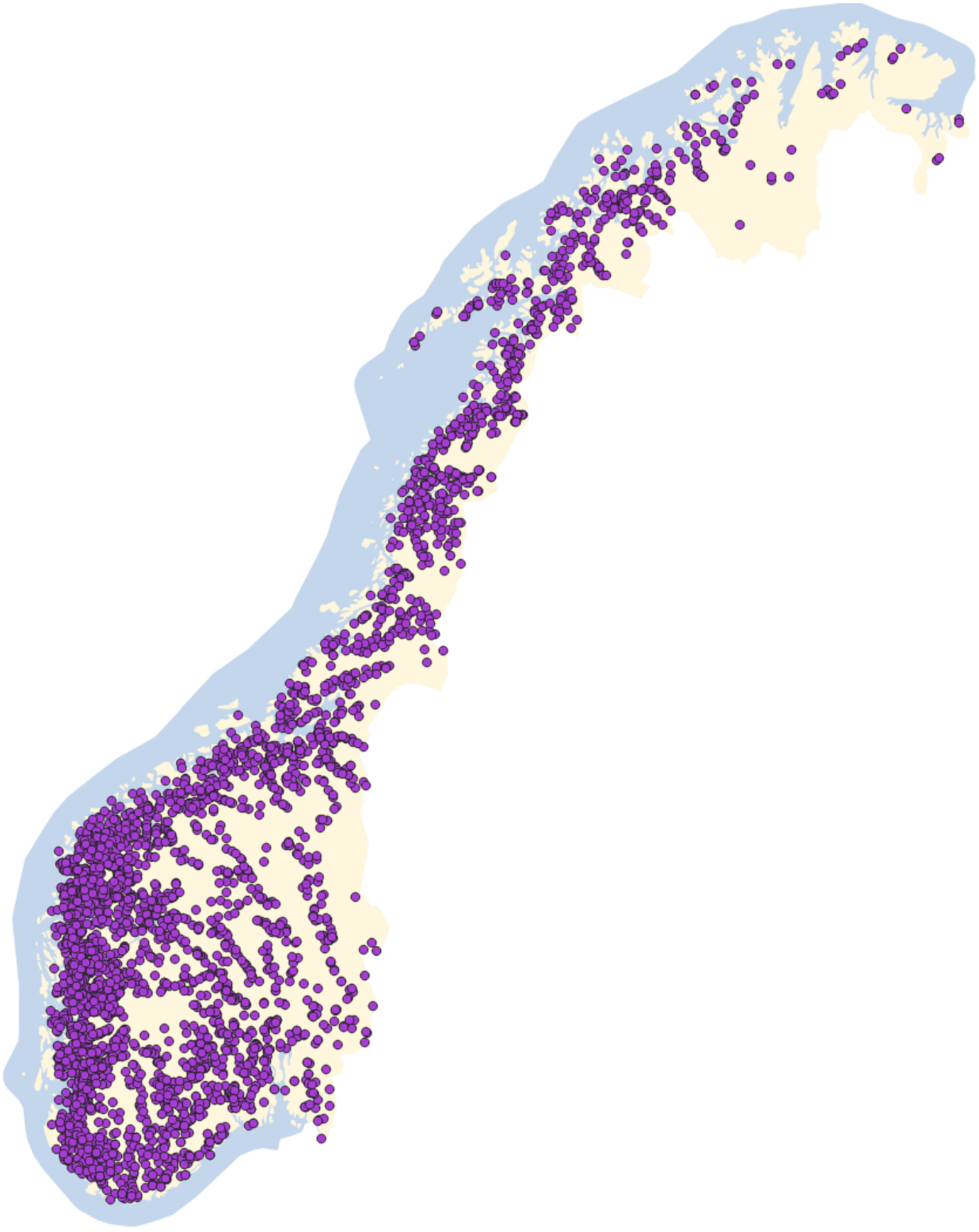

Figure 39: Map of Norwegian hydropower stations. Source: NVE (data) [46], The Norwegian Mapping Authority (background) [53].

Figure 40: Map of Norwegian electricity price areas. Source: NVE (data) [46], The Norwegian Mapping Authority (background) [53].

B Municipality centers for soiling estimations

Municipality	East UTM33	North UTM33
Stavanger	-25308.63	6589396.19
Oslo	262335.42	6656953.39
Trondheim	271498.57	7031656.93
Tromsø	658360.12	7730850.47
Bergen	-28836.01	6730622.71
Kristiansand	80506.37	6471393.70
Lillehammer	251868.28	6785781.36
Drammen	227320.62	6629577.22
Skien	185790.29	6581475.50
Tønsberg	232453.14	6590090.30
Fredrikstad	267715.29	6572429.07

Table 9: Municipality centers from Norwegian Mapping Authority [68]

Norges miljø- og biovitenskapelige universitet
Noregs miljø- og biovitskapelege universitet
Norwegian University of Life Sciences

Postboks 5003
NO-1432 Ås
Norway